

K-THEORY AND PSEUDOSPECTRA FOR TOPOLOGICAL INSULATORS

TERRY A. LORING

ABSTRACT. We derive formulas and algorithms for Kitaev's invariants in the periodic table for topological insulators and superconductors for finite disordered systems on lattices with boundaries. We find that K -theory arises as an obstruction to perturbing approximately compatible observables into compatible observables.

We derive formulas in all symmetry classes up to dimension two, and in one symmetry class in dimension three, that can be computed with sparse matrix algorithms. We present algorithms in two symmetry classes in 2D and one in 3D and provide illustrative studies regarding how these algorithms can detect the scaling properties of phase transitions.

1. APPROXIMATELY COMPATIBLE OBSERVABLES

Compatible observables are given by a rigid definition. If they act on finite Hilbert space, the requirement is a basis of vectors that are completely localized for each X_j , so $X_j \mathbf{v} = \lambda_j \mathbf{v}$ for some scalars. If we repeatedly prepare precisely the same state, we can hope to get no variance in whichever X_j we then measure. This sounds more like a math theory than any laboratory. What if we repeatedly prepare approximately the same state and approximately measure one of the X_j in turn, and each series of measurements shows little variation? Might this happen because the X_j are *approximately compatible*?

In the end, we expect this to mean the commutators $[X_j, X_k] = X_j X_k - X_k X_j$ are small, preferably in the operator norm. However the initial definition should involve something like small variance of states. More simply, we can seek common approximate eigenvectors. A fundamental quantity would seem to be, for an n -tuple of scalars $\lambda_1, \dots, \lambda_d$,

$$(1.1) \quad \min_{\|\mathbf{v}\|=1} \max_j \|X_j \mathbf{v} - \lambda_j \mathbf{v}\|.$$

If this quantity is small enough, often enough, we could declare these observables to be approximately compatible.

This seems like a nearly impossible minimization, so we seek a proxy. Commuting operators have a nice joint spectrum called the Clifford spectrum, so we apply the definition of Clifford spectrum to tuples of matrices with relatively small commutators and see what happens. The resulting joint spectrum has nice theoretical properties, a beautiful relation with K -theory, but remains difficult to compute numerically.

Generalizing pseudospectrum to what we call the Clifford pseudospectrum, we find an efficiently computable approximation to Equation 1.1.

Definition 1.1. Suppose X_1 through X_d are Hermitian matrices. Let $\Gamma_1, \dots, \Gamma_d$ be any Hermitian representation of the relations for $\mathcal{C}\ell_{d,0}(\mathbb{C})$, meaning $\Gamma_j^* = \Gamma_j$, $\Gamma_j^2 = 1$ and $\Gamma_j\Gamma_k = -\Gamma_k\Gamma_j$ for $j \neq k$. The *Clifford ϵ -pseudospectrum* of (X_1, \dots, X_d) is

$$\Lambda_\epsilon(X_1, \dots, X_d) = \left\{ \boldsymbol{\lambda} \in \mathbb{R}^d \mid \left\| \left(\sum (X_j - \lambda_j) \otimes \Gamma_j \right)^{-1} \right\| \geq \epsilon^{-1} \right\}$$

with the convention $0^{-1} = \infty$ and $\|S^{-1}\| = \infty$ whenever S is singular. The *Clifford spectrum* of (X_1, \dots, X_d) is $\Lambda_0(X_1, \dots, X_d)$, also denoted $\Lambda(X_1, \dots, X_d)$. The complement of the Clifford spectrum we call the *Clifford resolvent set*.

We will use the notation

$$B(X_1, \dots, X_d) = \sum X_j \otimes \Gamma_j$$

and

$$\begin{aligned} B_\lambda(X_1, \dots, X_d) &= B(X_1 - \lambda_1 I, \dots, X_n - \lambda_d I) \\ &= B(X_1, \dots, X_n) - B(\lambda I, \dots, \lambda_d I). \end{aligned}$$

For example,

$$\Lambda(X_1, \dots, X_d) = \left\{ \boldsymbol{\lambda} \in \mathbb{R}^d \mid B_\lambda(X_1, \dots, X_d) \text{ is singular} \right\}.$$

The representations of $\mathcal{C}\ell_{d,0}(\mathbb{C})$ are not complicated, so it is routine to show this definition does not depend on the choice of the Γ_j . When we get to K -theory we will need to keep the matrix size as small as possible to avoid multiplicity in the spectrum of $B_\lambda(X_1, \dots, X_n)$.

Lemma 1.2. *Suppose X_1, \dots, X_d are Hermitian n -by- n matrices. If $\boldsymbol{\lambda}$ is in $\Lambda_\epsilon(X_1, \dots, X_d)$ then there is a unit vector \mathbf{v} in \mathbb{C}^n with*

$$\|X_j \mathbf{v} - \lambda_j \mathbf{v}\| \leq \sqrt{\left\lceil \frac{d+1}{2} \right\rceil} \sqrt{\epsilon^2 + \sum_{j \neq k} \|[X_j, X_k]\|}$$

for all j .

Proof. Assume we have selected the Γ_j in $\mathbf{M}_g(\mathbb{C})$ where g is minimal, so $g = \lceil \frac{d+1}{2} \rceil$. Without loss of generality, we assume $\boldsymbol{\lambda}$ equals $\mathbf{0}$, and

$$\epsilon = \|(B(X_1, \dots, X_d)^{-1})^{-1}\|.$$

Since $B(X_1, \dots, X_d)$ is Hermitian, ϵ has the alternate description as the absolute value of the smallest eigenvalue of $B(X_1, \dots, X_d)$. Let \mathbf{z} be a corresponding unit eigenvector. Since

$$(1.2) \quad B(X_1, \dots, X_d)^2 = \sum_j X_j^2 \otimes I_g + \sum_{j \neq k} [X_j, X_k] \otimes \Gamma_j \Gamma_k$$

we make the estimate

$$\begin{aligned} \left\| \left(\sum X_j^2 \otimes I_g \right) \mathbf{z} \right\| &\leq \|B(X_1, \dots, X_d)^2 \mathbf{z}\| + \left\| \left(\sum_{j \neq k} [X_j, X_k] \otimes \Gamma_j \Gamma_k \right) \mathbf{z} \right\| \\ &\leq \epsilon^2 + \sum_{j \neq k} \|[X_j, X_k]\|. \end{aligned}$$

Let

$$\mathbf{z} = \begin{bmatrix} \mathbf{z}_1 \\ \vdots \\ \mathbf{z}_g \end{bmatrix}$$

and let r be an index maximizing $\|\mathbf{z}_r\|$, so we have $\|\mathbf{z}_r\| \geq 1/g$. Let $\mathbf{v} = \mathbf{z}_r / \|\mathbf{z}_r\|$. Since

$$\left\| \sum X_j^2 \mathbf{z}_r \right\| \leq \left\| \left(\sum X_j^2 \otimes I_g \right) \mathbf{z} \right\|$$

we have

$$\left\| \sum X_j^2 \mathbf{v} \right\| \leq g \left\| \left(\sum X_j^2 \otimes I_g \right) \mathbf{z} \right\|.$$

Since $X_\ell^2 \leq \sum_j X_j^2$ we find

$$\langle X_\ell^2 \mathbf{v}, \mathbf{v} \rangle \leq \left\langle \sum_j X_j^2 \mathbf{v}, \mathbf{v} \right\rangle \leq \left\| \sum_j X_j^2 \mathbf{v} \right\|$$

and so

$$\langle X_\ell^2 \mathbf{v}, \mathbf{v} \rangle \leq g \left(\epsilon^2 + \sum_{j \neq k} \|[X_j, X_k]\| \right).$$

□

Lemma 1.3. *Suppose X_1, \dots, X_d are Hermitian n -by- n matrices. If*

$$\|X_j \mathbf{v} - \lambda_j \mathbf{v}\| \leq \epsilon$$

for all j , then $\boldsymbol{\lambda}$ is in $\Lambda_{\epsilon'}(X_1, \dots, X_d)$ where

$$\epsilon' = \sqrt{\left| \frac{d+1}{2} \right|^{\frac{1}{2}} d \epsilon^2 + \sum_{j \neq k} \|[X_j, X_k]\|}.$$

Proof. Again we use linearity to reduce to the case $\boldsymbol{\lambda} = \mathbf{0}$. If $\|X_j \mathbf{v}\| \leq \epsilon$ for all j then let

$$\mathbf{z} = \begin{bmatrix} \mathbf{v} \\ \vdots \\ \mathbf{v} \end{bmatrix}.$$

Using Equation 1.2 we find

$$\begin{aligned}
\|(B(X_1, \dots, X_d))^2 \mathbf{z}\| &\leq \left\| \left(\sum_j X_j^2 \otimes I_g \right) \mathbf{z} \right\| + \sum_{j \neq k} \|[X_j, X_k]\| \\
&= \sqrt{g} \left\| \sum_j X_j^2 \mathbf{v} \right\|^2 + \sum_{j \neq k} \|[X_j, X_k]\| \\
&\leq \sqrt{g} \sum_j \|X_j^2 \mathbf{v}\| + \sum_{j \neq k} \|[X_j, X_k]\| \\
&\leq \sqrt{gd}\epsilon^2 + \sum_{j \neq k} \|[X_j, X_k]\|.
\end{aligned}$$

This gives a lower bound on the norm of $(B(X_1, \dots, X_d))^2$, specifically

$$\|(B(X_1, \dots, X_d))^{-2}\| \geq \left(\sqrt{gd}\epsilon^2 + \sum_{j \neq k} \|[X_j, X_k]\| \right)^{-1}.$$

Since $B(X_1, \dots, X_d)$ is Hermitian, we conclude

$$\|(B(X_1, \dots, X_d))^{-1}\|^{-1} \leq \sqrt{\sqrt{gd}\epsilon^2 + \sum_{j \neq k} \|[X_j, X_k]\|}.$$

□

Remark 1.4. Lemmas 1.2 and 1.3 tell us that for almost commuting Hermitian matrices X_1, \dots, X_d we can get an approximation to the quantity in Equation 1.1 by computing

$$\|(B_\lambda(X_1, \dots, X_d))^{-1}\|^{-1}.$$

In a numerical setting, we can compute this easily. For example, we can compute the absolute value of the eigenvalue of $B(X_1, \dots, X_d)$ that is closest to zero. This matrix is Hermitian, and typically sparse, so standard algorithms work well for modest matrix sizes. The algorithms typically compute an associated (approximate) eigenvalue, so we have a way to construct vectors that come close to the minimum in Equation 1.1. As we push the matrix sizes larger, we will need to do better. Still, estimating the norm of an inverse is a fairly standard problem in numerical analysis. One issue is that it is hard to differentiate an eigenvalue at zero from one close to zero. This is why we turn to the pseudospectrum. If we are computing the function

$$\lambda \mapsto \|(B_\lambda(X_1, \dots, X_d))^{-1}\|^{-1}$$

we need to set a value ϵ just above zero and regard all values below that as equal. This is very reasonable, as we are modeling simultaneous approximate measurement when true simultaneous measurement is impossible.

Example 1.5. If X_1, \dots, X_d are commuting Hermitian matrices then $\Lambda(X_1, \dots, X_d)$ equals the usual joint spectrum. This is an immediate corollary of Lemma 1.2 and Lemma 1.3.

Example 1.6. If A and B are Hermitian, then (λ_1, λ_2) is in $\Lambda(A, B)$ if and only if $\lambda_1 + i\lambda_2$ is in the spectrum of $A + iB$. So the Clifford spectrum of a pair of Hermitian matrices is finite. For positive ϵ we can show that (λ_1, λ_2) is in $\Lambda_\epsilon(A, B)$ if and only if $\lambda_1 + i\lambda_2$ is in the usual pseudospectrum of $A + iB$. However need the convention

$$\sigma_\epsilon(Y) = \{ \alpha \in \mathbb{C} \mid \|(\alpha - Y)^{-1}\| \geq \epsilon^{-1} \}$$

and not the convention with strict inequality, as in the excellent book [37] by Trefethen and Embree. To see the connection, we temporarily use

$$\Gamma_1 = \begin{bmatrix} 0 & 1 \\ 1 & 0 \end{bmatrix}, \quad \Gamma_2 = \begin{bmatrix} 0 & i \\ -i & 0 \end{bmatrix}$$

so that

$$-B_{(\lambda_1, \lambda_2)}(A, B) = \begin{bmatrix} 0 & (\lambda_1 + i\lambda_2) - (A + iB) \\ ((\lambda_1 + i\lambda_2) - (A + iB))^* & 0 \end{bmatrix}.$$

Often the better choices here are

$$\Gamma_1 = \begin{bmatrix} 0 & 1 \\ 1 & 0 \end{bmatrix}, \quad \Gamma_2 = \begin{bmatrix} 1 & 0 \\ 0 & -1 \end{bmatrix}$$

as this keeps

$$B_{(\lambda_1, \lambda_2)}(A, B) = \begin{bmatrix} B - \lambda_2 & A - \lambda_1 \\ A - \lambda_1 & -B + \lambda_2 \end{bmatrix}$$

real when A and B are real. Then we are able to produce real joint approximate eigenvalues for A and B by finding near null vectors of $B_{(\lambda_1, \lambda_2)}(A, B)$.

Next an example where the Clifford spectrum is an infinite set. For $d = 3$ the clear choice for the Γ_j is $\Gamma_1 = \sigma_x$, $\Gamma_2 = \sigma_y$, $\Gamma_3 = \sigma_z$ so that

$$B(X, Y, Z) = \begin{bmatrix} Z & X - iY \\ X + iY & -Z \end{bmatrix}$$

as was done in previous work with Hastings [17].

Example 1.7. A nice example, computed by Kisil [21], shows us that the Clifford spectrum for three Hermitian matrices is radically different from the Clifford spectrum of two Hermitian matrices (as defined below), as it need not be a finite set. We compute $\Lambda(\sigma_x, \sigma_y, \sigma_z)$ with help from a symbolic algebra package. The ‘‘characteristic

polynomial" here is

$$\begin{aligned} & \det(B(\sigma_x - rI, \sigma_y - sI, \sigma_z - tI)) \\ &= \det \left(\begin{bmatrix} 1-t & 0 & -r+is & 0 \\ 0 & -1-t & 2 & -r+is \\ -r-is & 2 & -1+t & 0 \\ 0 & -r-is & 0 & 1+t \end{bmatrix} \right) \\ &= (r^2 + s^2 + t^2 + 1)^2 - 4. \end{aligned}$$

This means $\Lambda(\sigma_x, \sigma_y, \sigma_z)$ is the unit sphere.

While investigating D-branes, Berenstein Malinowski [3] took the preceding example further. In that setting, the position observables do not commute. They looked at higher spin representations and computed the Clifford spectrum, again a sphere. In fact they were interested in a subset of the Clifford spectrum that needs some form of K -theory for its definition.

Where an index, and eventually K -theory, arise is easily seen in Example 1.7. Let us examine what is going on at two points in the Clifford resolvent set, the origin and $(0, 0, 2)$. We find that

$$B_{\mathbf{0}}(\sigma_x, \sigma_y, \sigma_z) = \begin{bmatrix} 1 & 0 & 0 & 0 \\ 0 & -1 & 2 & 0 \\ 0 & 2 & -1 & 0 \\ 0 & 0 & 0 & 1 \end{bmatrix}$$

which has a single eigenvalue at -3 and a triple eigenvalue at 1 . On the other hand

$$B_{(0,0,2)}(\sigma_x, \sigma_y, \sigma_z) = \begin{bmatrix} -3 & 0 & 0 & 0 \\ 0 & -3 & 2 & 0 \\ 0 & 2 & 1 & 0 \\ 0 & 0 & 0 & 3 \end{bmatrix}$$

has spectrum

$$\{-1 - \sqrt{8}, -1, -1 + \sqrt{8}, 3\}$$

and so the same number of positive and negative eigenvalues. As we vary $\boldsymbol{\lambda}$ the eigenvalues move continuously. It follows that for any $\boldsymbol{\lambda}$ inside the unit sphere $B_{\boldsymbol{\lambda}}(\sigma_x, \sigma_y, \sigma_z)$ will have just one positive eigenvalue. For $\boldsymbol{\lambda}$ outside the unit sphere $B_{\boldsymbol{\lambda}}(\sigma_x, \sigma_y, \sigma_z)$ will have exactly two positive eigenvalues. The Clifford resolvent set contains information and we will see that from a computation of $B_{\boldsymbol{\lambda}}(X_1, \dots, X_d)$ at a single point we can make predictions on the size of the Clifford spectrum. This is the mathematical essence of bulk-edge correspondence.

We now require that our Γ_j are selected in matrices of minimal size. In fact, let us consider $d = 3$ and use the Pauli spin matrices, as above. Recall that for an invertible Hermitian matrix Q the *signature* of Q is the number of positive eigenvalues (with

multiplicity) minus the number of negative eigenvalues of Q , denoted $\text{Sig}(Q)$. Note the signature is always even for even size matrices.

Definition 1.8. If λ is not in $\Lambda(X, Y, Z)$ then the index of this triple at λ is

$$\text{Ind}_\lambda(X, Y, Z) = \frac{1}{2} \text{Sig}(B_\lambda(X, Y, Z))$$

which is in the abelian group \mathbb{Z} .

Remark 1.9. We use primarily the notation of pure mathematics. In particular $*$ indicates the conjugate transpose of a matrix, and is a special instance of the $*$ operation in a C^* -algebra.

Example 1.10. Consider a finite model of a two-dimensional Chern insulator on square lattice. That is, with zero for boundary conditions. The Hamiltonian we consider a tight binding model, where there are two orbital types at each site on a square lattice. We have creation operators $c_{m,n,P}$ and $c_{m,n,S}$ at site (m, n) in band P or S. Let $c_{m,n}$ be the sum of these two types of create at the same site. The periodic Hamiltonian is

$$\begin{aligned} H_{\text{per}} = & \sum_{m,n} c_{m,n}^* (-\sigma_z - \sigma_y) c_{m+1,n} + h.c. \\ & + \sum_{m,n} c_{m,n}^* (-\sigma_z - i\sigma_y) c_{m,n+1} + h.c. \\ & + \sum_{m,n} c_{m,n}^* ((3 + \mu_{m,n}) \sigma_z) c_{m,n} \end{aligned}$$

where $\mu_{m,n}$ is drawn with uniform distribution from $[-\frac{N}{2}, \frac{N}{2}]$ where N sets the disorder level. This is the model used for a Chern insulator as part of the numerical study done with Hastings [29], which was essentially the spin-up only part of the model for an HgTe quantum wells given in [24]. If we use lattice position (roughly Ångströms) in defining our position operators, we find $\|[H, X]\|$ and $\|[H, Y]\|$ rather large, about 6. We work with the triple $(\eta X, \eta Y, H)$, although we plot our results using lattice units. For this example, $\eta = 0.5$ was selected as a value for which the computed approximate eigenvectors we spread out roughly one nanometer in position. We calculated the ϵ -pseudospectrum, and also the index at many positions at the Fermi level. For better viewing, the X coordinate of the λ was truncated to $[-2, 2]$ and energy coordinate to $[-2.5, 2.5]$. The full energy spectrum is roughly $[-7, 7]$. This portion of the pseudospectrum and labeled resolvent is shown in Figures 1.1-1.3 with an increasingly large random disorder. The pseudospectrum is calculated at 5 grid points per unit and $\epsilon = 0.05$.

2. ALMOST COMMUTING MATRICES, THE TEN-FOLD WAY

We have many potential sources of almost commuting matrices, but now focus on situations most relevant to topological insulators. A lattice model of a D -dimensional

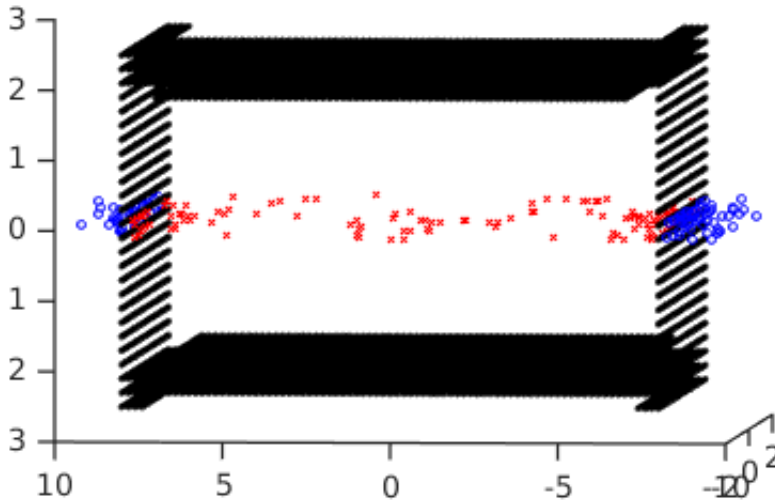


FIGURE 1.1. A Chern insulator on a 18-by-18 lattice with no disorder.

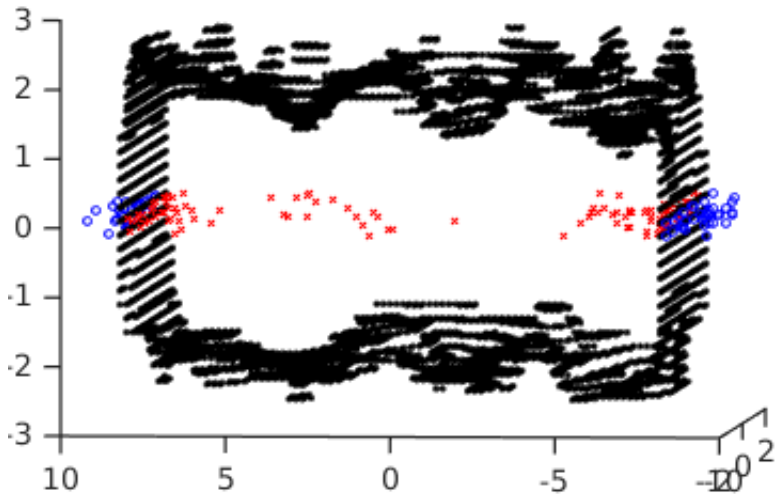


FIGURE 1.2. A Chern insulator on a 18-by-18 lattice with disorder at 4.

topological or ordinary insulator needs $D+1$ Hermitian matrices to be described. The D position operators X_j will commute with each other and almost commute with the Hamiltonian H . In most situations our formulas will work just as well if the X_j almost commute, so we do not always require the X_j to exactly commute.

We now consider the ten symmetry classes in the Atland-Zirnbauer [1] classification. Depending on the symmetry class, we may have up to three symmetries. Time reversal will be denoted \mathcal{T} and be antiunitary and commute with all $D+1$ matrices. Particle-hole conjugation will also be anti-unitary, will commute with position and anticommute with the Hamiltonian. The symmetry S will be unitary, commute with

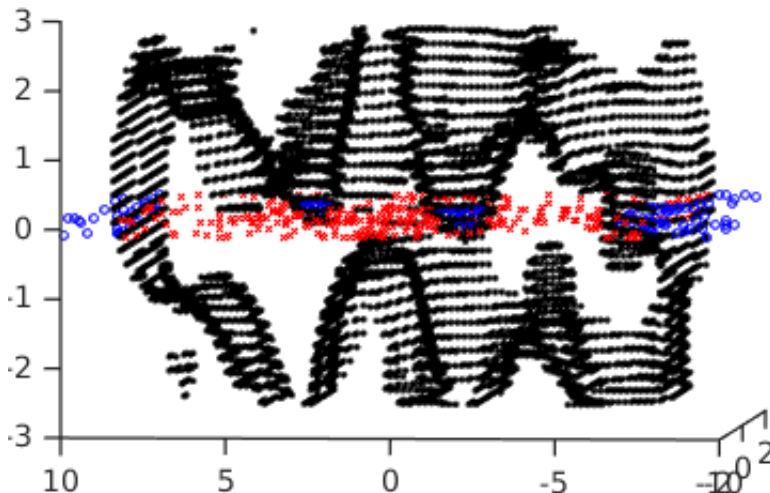


FIGURE 1.3. A Chern insulator on a 18-by-18 lattice with disorder at 10.

position and anticommute with H . If all three are present, then S is the product of the other two, which commute. All symmetries are of order two.

Following Kitaev [22], we will focus on situations where there is a localized spectral gap. A minimal interpretation of this is

$$\mathbf{0} \notin \Lambda(X_1, \dots, X_D, H).$$

However, we are dealing with approximate measurement, so a better definition is generally

$$\|B(X_1, \dots, X_D, H)^{-1}\| \leq \delta_1$$

and $\|[X_j, X_k]\| \leq \delta_2$ and $\|[X_j, H]\| \leq \delta_2$. For each choice of δ_1 and δ_2 we are specifying a potentially useful collection of systems.

In lower dimensions we can hope to classify such systems up to homotopy and identify computable invariants to detect these homotopy classes. As we move to higher dimensions we need to allow for stabilization by adding on trivial systems.

In addition to homotopy questions, we can ask of a given system is close to another system that is in the atomic limit, where the Hamiltonian commutes with all the position operators. This is then a special case of a mathematical question. Given $D + 1$ almost commuting Hermitian matrices X_1, \dots, X_{D+1} in specific AZ class that almost commute, are there nearby commuting Hermitian matrices in the same class that commute. To be a serious question this must be posed in a way that is uniform for all matrix sizes. That is, in Theorem 2.1 the selected δ must work for all choices for the matrix size n .

One instance of this, for dimension 2 in class D, asks the following. Given two real symmetric and one imaginary antisymmetric matrices that almost commute, can these can be uniformly approximated by commuting matrices, again with two

Cartan class	\mathcal{T}	\mathcal{C}	S
<i>Complex</i>			
A	—	—	—
AIII	—	—	✓
<i>Real</i>			
AI	$\mathcal{T} \circ \mathcal{T} = I$	—	—
BDI	$\mathcal{T} \circ \mathcal{T} = I$	$\mathcal{C} \circ \mathcal{C} = I$	✓
D	—	$\mathcal{C} \circ \mathcal{C} = I$	—
DIII	$\mathcal{T} \circ \mathcal{T} = -I$	$\mathcal{C} \circ \mathcal{C} = I$	✓
AII	$\mathcal{T} \circ \mathcal{T} = -I$	—	—
CII	$\mathcal{T} \circ \mathcal{T} = -I$	$\mathcal{C} \circ \mathcal{C} = -I$	✓
C	—	$\mathcal{C} \circ \mathcal{C} = -I$	—
CI	$\mathcal{T} \circ \mathcal{T} = I$	$\mathcal{C} \circ \mathcal{C} = -I$	✓

TABLE 1. The symmetry classes. The mark ✓ means this symmetry exists, and $SHS = -H$ and $SX_jS = X_j$ for a unitary S , with H the Hamiltonian and X_j any of the position observables. The mark — means this symmetry does not exist. If the other two symmetries exist then $S = \mathcal{T} \circ \mathcal{C} = \mathcal{C} \circ \mathcal{T}$. All other formulas indicate the symmetry exists, with the stated conditions holding, with $SHS = -H$ and $SX_jS = X_j$, or $\mathcal{T} \circ H = H \circ \mathcal{T}$ and $\mathcal{T} \circ X_j = X_j \circ \mathcal{T}$, or $\mathcal{C} \circ H = -H \circ \mathcal{C}$ and $\mathcal{C} \circ X_j = X_j \circ \mathcal{C}$.

Cartan class	Dimension							
	0	1	2	3	4	5	6	7
<i>Complex</i>								
A	\mathbb{Z}	0	\mathbb{Z}	0	\mathbb{Z}	0	\mathbb{Z}	0
AIII	0	\mathbb{Z}	0	\mathbb{Z}	0	\mathbb{Z}	0	\mathbb{Z}
<i>Real</i>								
AI	\mathbb{Z}	0	0	0	\mathbb{Z}	0	\mathbb{Z}_2	\mathbb{Z}_2
BDI	\mathbb{Z}_2	\mathbb{Z}	0	0	0	\mathbb{Z}	0	\mathbb{Z}_2
D	\mathbb{Z}_2	\mathbb{Z}_2	\mathbb{Z}	0	0	0	\mathbb{Z}	0
DIII	0	\mathbb{Z}_2	\mathbb{Z}_2	\mathbb{Z}	0	0	0	\mathbb{Z}
AII	\mathbb{Z}	0	\mathbb{Z}_2	\mathbb{Z}_2	\mathbb{Z}	0	0	0
CII	0	\mathbb{Z}	0	\mathbb{Z}_2	\mathbb{Z}_2	\mathbb{Z}	0	0
C	0	0	\mathbb{Z}	0	\mathbb{Z}_2	\mathbb{Z}_2	\mathbb{Z}	0
CI	0	0	0	\mathbb{Z}	0	\mathbb{Z}_2	\mathbb{Z}_2	\mathbb{Z}

TABLE 2. The range of the invariants [23, 35].

being real symmetric and being imaginary antisymmetric. The answer is no, with an obstruction in \mathbb{Z} , as indicated in table 2.

We tend to prefer describing the symmetries in terms of operations on matrices [27]. So we work with the dual operation \sharp that is derived from fermionic time-reversal by

$$Q^\sharp = \mathcal{T}^{-1} \circ Q^* \circ \mathcal{T}$$

were

$$\mathcal{T} \begin{bmatrix} \mathbf{v} \\ \mathbf{w} \end{bmatrix} = \begin{bmatrix} -\overline{\mathbf{w}} \\ \overline{\mathbf{v}} \end{bmatrix}.$$

In block form,

$$\begin{bmatrix} A & B \\ C & D \end{bmatrix}^\sharp = \begin{bmatrix} D^\top & -B^\top \\ -C^\top & A^\top \end{bmatrix}.$$

The first two columns in Table 2 are unique. These invariants are just a reflection of the homotopy classes of such locally-gapped systems. In these columns the invariants do not represent obstructions to a system being close to another system in the atomic limit. The mathematics behind this statement is nontrivial. It says that approximately measuring two incompatible observables simultaneously is very different from doing so with three or more.

Theorem 2.1. (Lin's Theorem, 1995) *For any $\epsilon > 0$, there exists $\delta > 0$ such that whenever $n \in \mathbb{N}$ and two self-adjoint matrices H and X in $\mathbf{M}_n(\mathbb{C})$ satisfy $\|H\| \leq 1$ and $\|X\| \leq 1$ and*

$$\|HX - XH\| \leq \delta,$$

there exists a pair of self-adjoint matrices H_1 and X_1 in $\mathbf{M}_n(\mathbb{C})$ such that

$$\|H_1 - H\| \leq \epsilon, \quad \|X_1 - X\| \leq \epsilon$$

and $H_1 X_1 = X_1 H_1$.

Lin's original proof [26] is difficult, so perhaps a better starting point in the literature is [13]. However, Ogata [33] adapted Lin's original proof to work with more than two almost commuting Hermitian matrices in a special case involving macroscopic observables. These observables are multiparticle averages that avoid the K -theory in columns two and above in Table 2.

Conjecture 2.2. *Lin's Theorem remains true if we assume that (X, H) is in any Atland-Zirnbauer symmetry class and we require that (X_1, H_1) be in the same symmetry class.*

Joint work with Sørensen [30, 31] proved that this conjecture is valid in classes AI, D, AII and C. Of course Lin dealt with class A, leaving the conjecture open on the five classes involving two antiunitary symmetries. Even in the complex case, research into Lin's theorem is not over, in particular looking at quantitative versions, as in [16, 19].

The only serious consequence of Lin's theorem we explore here is the following remark about 1D systems. However, there are expected to be results regarding the classification of 2D systems, along the lines of the results in [31].

Remark 2.3. Consider two almost commuting Hermitian operators H and X . The Clifford spectrum of this pair will be a perturbation of the Clifford spectrum of a commuting pair, which is a finite set. The Clifford pseudo spectrum computed for 1D systems has typically been a collection of small disconnected regions. The computations done have been limited, but it is expected that the pseudo spectrum of a 1D system look very different from the mutated spheres we see for 2D systems.

3. DIMENSION ZERO, INDEX FORMULAS

Many approaches to the K -theory of topological insulators rely on spectrally flattened Hamiltonian, or equivalently the Fermi projector. For example, see [2, 11, 32, 34]. One approach that avoids this is the scattering matrix approach [14, 36]. There are many numerical issues related to working with matrices with high degeneracy in the spectrum, so we prefer to work directly with the full class of invertible Hermitian matrices.

The homotopy classification in dimension zero is rather standard. However the formulas for the invariants are not all standard. Our invariants are only designed to work for finite models, but it is anticipated that there will be connections with indexes defined to work in infinite volume, such as [10, 32, 34].

Theorem 3.1. *In each of the ten Atland-Zirnbauer symmetry classes, two invertible n -by- n Hermitian matrices are homotopic via invertibles in that class if and only if the values of an index (in the group 0 or \mathbb{Z} or \mathbb{Z}_2) for each matrix are equal. This index can be computed in $O(n^3)$ time. The index for each class is listed below.*

An important consideration is how these invariants can be computed more quickly than $O(n^3)$ when the matrices are sparse. We will give brief remarks on sparse algorithms below.

3.1. Class A in 0D. There are no symmetries, except $H = H^*$ in $GL_n(\mathbb{C})$. The index is

$$\frac{1}{2}\text{Sig}(H)$$

and it is just a variation on the spectral theorem that this classifies such matrices up to homotopy.

Remark 3.2. The signature can be computed using the LDLT decomposition, which finds a unit lower triangular matrix L and a block diagonal matrix D with 1-by-1 and 2-by-2 blocks so that $H = LDL^*$. By Sylvester's law of inertia, $\text{Sig}(H) = \text{Sig}(D)$ and the signature of D can be found in linear time. Since $LDLT$ is $O(n^3)$ we are done in this case. If H is sparse, there is a readily available sparse version of the LDLT algorithm [7].

3.2. Class AI in 0D. We now have H real. We can view that as the added symmetry $H^T = H$. The index is again

$$\frac{1}{2}\text{Sig}(H)$$

and the algorithms mentioned in §3.1 are available also in the real case. The essential fact in proving that this invariant classifies is that H can be factored as $H = U^*DU$ with D diagonal with decreasing diagonal terms and U being real orthogonal with determinant one.

3.3. Class BDI in 0D. The symmetries here can be taken to be $H^T = H$ and $H\Gamma = -\Gamma H$ for $H = H^*$ in $\text{GL}_n(\mathbb{C})$ with

$$\Gamma = \begin{bmatrix} I & 0 \\ 0 & -I \end{bmatrix}.$$

That is,

$$H = \begin{bmatrix} 0 & C \\ C^T & 0 \end{bmatrix}$$

for C an invertible real matrix. The index in this case is

$$\text{sign}(\det(C))$$

in $\mathbb{Z}_2 = \{\pm 1\}$. Recall that two real invertible matrices can be path connected if and only if their determinants are of the same sign.

Remark 3.3. There is a noncanonical choice to be made here, specifically a real unitary from $\mathbb{C}^n \oplus 0 \mapsto 0 \oplus \mathbb{C}$.

Remark 3.4. The sign of the determinant can be computed using the LU decomposition, which finds a lower triangular matrix L and an upper triangular matrix R so that $C = LR$. Then

$$\text{sign}(\det(C)) = \prod \text{sign}(L_{jj}) \prod \text{sign}(R_{jj})$$

which avoids the underflow and overflow associated with computing determinants of large matrices. Since LU is $O(n^3)$ we are done in this case. If H is sparse, there are readily available sparse versions of the LU algorithm [6].

3.4. Class D in 0D. The symmetry here can be taken to be $H^T = -H$ for $H = H^*$ in $\text{GL}_{2n}(\mathbb{C})$. The eigenvalues of the real, normal matrix iH will come in conjugate pairs so its determinant is positive. This makes the Pfaffian real, and our invariant is

$$\text{sign}(\text{Pf}(iH)).$$

The homotopy classification can be understood here in terms of the factorization [18, Theorem 9.4] of H as $H = UDU^*$ where U is real orthogonal and D is diagonal.

Remark 3.5. The sign of the Pfaffian of $K = iH$ can be computed using a decomposition $K = LDL^T$ where D is tridiagonal. If H is banded, which will happen when working with derived Hamiltonians based on 1D systems, one can use software for

Pfaffians by Wimmer [38]. There is an algorithm, but no available software, for the more general case of sparse, real skew-symmetric matrices [8].

3.5. **Class AII, 0D.** We now have H self-dual, so $H^* = H^\sharp = H$. The index is

$$\frac{1}{4} \text{Sig}(H)$$

due to Kramer's doubling. The homotopy classification is best understood here in terms of the factorization of [18, Theorem 4.6], $H = UDU^*$ where U is a symplectic unitary and D is diagonal with $D_{j,j} = D_{j+n,j+n}$.

4. DIMENSION ONE, INDEX FORMULAS

Although Lin's theorem is deep, we can avoid it when we have two incompatible observables if we are willing to study systems up to homotopy. Given H and X Hermitian matrices, one form of our local gap condition

$$\begin{bmatrix} 0 & (X + iH)^* \\ X + iH & 0 \end{bmatrix} \text{ is invertible}$$

translates to the condition $W = X + iH$ is invertible. It is easy to deform an invertible to a unitary by the path

$$W_t = W (W^*W)^t$$

for t in $[0, 1]$. Extracting the Hermitian and anti-Hermitian parts $X_t = \frac{1}{2}W_t^* + \frac{1}{2}W_t$ and $H_t = \frac{i}{2}W_t^* - \frac{i}{2}W_t$ we get a path to a system the atomic limit. At all points on the path the commutator $[X_t, H_t]$ will remain small if the initial commutator is assumed sufficiently small. One can check that this construction respects the various symmetries. For example, in class C we have $H^\sharp = -H$ and $X^\sharp = -X$. This implies $W^\sharp = W^*$. Functional calculus commutes with \sharp so

$$(W_t)^\sharp = (W^*W)^t W^* = (W_t)^*.$$

Finally

$$X_t^\sharp = \frac{1}{2}W_t^* + \frac{1}{2}W_t = X_t$$

and

$$H_t^\sharp = \frac{1}{2}W_t + \frac{1}{2}W_t^* = -H_t.$$

By this homotopy argument, we can simply check that a formula is invariant under homotopy and that correctly classifies systems in the atomic limit, at least up to homotopy.

4.1. **Class AIII in 1D** . We can assume we have $H = H^*$ and $X = X^*$ in $\mathbf{M}_n(\mathbb{C})$, with $X + iH$ assumed to be invertible. With

$$\Gamma = \begin{bmatrix} I & 0 \\ 0 & -I \end{bmatrix}$$

defining a grading, we have $H\Gamma = -\Gamma H$ and $X\Gamma = \Gamma X$. This means that $(X + iH)\Gamma$ is Hermitian. It is invertible because Γ is unitary. The index we use here is

$$\frac{1}{2}\text{Sig}((X + iH)\Gamma).$$

Consider the case where $W = X + iH$ is unitary, in this class. This means $U^\sigma = U$ where σ denotes conjugation by Γ . This symmetry will hold also for $f(U)$ so long as $f(\bar{\lambda}) = f(\lambda)$. We can select a vertical line in the complex plane, near the imaginary axis, that misses the spectrum of U and get a homotopy f_t from the identity function to the function that maps all to the right of the line to 1 and all to the left to -1 . Thus we have a homotopy to a unitary that is symmetric. Back in the X and H picture, we can assume $H = 0$. Along with the fact that X is even, we are in the situation

$$X = \begin{bmatrix} A & 0 \\ 0 & B \end{bmatrix}$$

where A and B are Hermitian. Since $H = 0$ the index is

$$\frac{1}{2}\text{Sig}(A) - \frac{1}{2}\text{Sig}(B).$$

The reason this is the correct index to classify, where it seems we need two indices, is that we can bring back nonzero H and use paths such as

$$U_t = \begin{bmatrix} \cos(t) & & \sin(t) & & \\ & 1 & & 0 & \\ & & \ddots & & \ddots \\ \sin(t) & & & -\cos(t) & \\ & 0 & & & -1 \\ & & \ddots & & \ddots \end{bmatrix}$$

to increase the signature of B by t while decreasing the signature of A by the same amount.

4.2. **Class BDI in 1D**. We can assume H is odd and real and X is even and real, where even and odd is determined by the grading operator

$$\Gamma = \begin{bmatrix} I & 0 \\ 0 & -I \end{bmatrix}.$$

We can use the index from §4.1, but that turns out to be slower to compute that is necessary.

Example 4.1. Suppose α is real, between -1 and 1 , and set $\beta = \sqrt{1 - \alpha^2}$. Our example has

$$X = \begin{bmatrix} \alpha & 0 \\ 0 & \alpha \end{bmatrix}$$

and

$$H = \begin{bmatrix} 0 & \beta \\ \beta & 0 \end{bmatrix}.$$

These have the correct symmetries, and

$$(X + iH)\Gamma = \begin{bmatrix} \alpha & -i\beta \\ i\beta & \alpha \end{bmatrix}.$$

This has signature 0. It is unitarily equivalent to a real matrix, which is not an accident.

We use the unitary $Q = \omega I + \bar{\omega}\Gamma$ where $\omega = \frac{1}{2} - \frac{i}{2}$. We can conjugate by a unitary matrix without altering the signature, and we compute

$$\begin{aligned} Q(X + iH)\Gamma Q^* &= (\omega I + \bar{\omega}\Gamma)(X + iH)\Gamma(\bar{\omega}I + \omega\Gamma) \\ &= X\Gamma + H \end{aligned}$$

and discover a nice index,

$$\frac{1}{2}\text{Sig}(X\Gamma + H)$$

which involves now the signature of a real symmetric matrix. See Remark 3.2 on computing signature, especially for sparse matrices.

The proof here that this invariant suffices is almost identical to the argument in Section 4.1.

4.3. Class D in 1D. Since $\mathcal{C}^2 = I$ we can assume $H^T = -H$ and $X^T = X$. Since these are Hermitian, we see X is real and H is pure-imaginary, so $X + iH$ is real. We are assuming it to be invertible. The index here is

$$\text{sign}(\det(X + iH)).$$

We know the sign of the determinant classifies real orthogonal matrices up to homotopy. We apply this to $X + iH$ and extract the needed Hermitian and anti-Hermitian parts.

4.4. Class DIII, 1D. We can assume H is imaginary and self-dual, and X is real and self-dual, but in this case we find that even and odd are to be determined by the grading operator

$$\Gamma = \begin{bmatrix} 0 & -iI \\ iI & 0 \end{bmatrix}.$$

This ensures that the transpose is conjugated to the dual. We use the unitary $Q = \omega I + \bar{\omega}\Gamma$ where $\omega = \frac{1}{2} - \frac{i}{2}$. We compute

$$\begin{aligned} Q(X + iH)\Gamma Q^* &= (\omega I + \bar{\omega}\Gamma)(X + iH)\Gamma(\bar{\omega}I + \omega\Gamma^*) \\ &= (\omega I + \bar{\omega}\Gamma)(X + iH)(\bar{\omega}\Gamma + \omega I) \\ &= -\frac{i}{2}(X + iH) + \frac{1}{2}\Gamma(X + iH) + \frac{1}{2}(X + iH)\Gamma + \frac{i}{2}\Gamma(X - iH)\Gamma \\ &= X\Gamma + H \end{aligned}$$

and we check its symmetries

$$(X\Gamma + H)^* = (\Gamma)X + H = (X\Gamma + H)$$

and since Γ and H are imaginary and X real, this is imaginary, and so skew-symmetric. We can compute a Pfaffian, as before, and our index is

$$\text{sign}(\text{Pf}(i(X\Gamma + H))).$$

Here is a sketch of why this invariant classifies. As in class AIII we are able to use functional calculus to reduce first to the case of $X + iH$ being unitary and then also to where $H = 0$. If X is real symmetric and self-dual and unitary, it can be shown that it will factor as

$$Q^* \begin{bmatrix} D & \\ & D \end{bmatrix} Q$$

with Q real orthogonal and symplectic and

$$D = \begin{bmatrix} 1 & & & & & \\ & \ddots & & & & \\ & & 1 & & & \\ & & & -1 & & \\ & & & & \ddots & \\ & & & & & -1 \end{bmatrix}.$$

To see how to finish the classification, notice the invariant comes out differently on

$$X_+ = \begin{bmatrix} 1 & \\ & 1 \end{bmatrix}, \quad X_- = \begin{bmatrix} -1 & \\ & -1 \end{bmatrix}$$

since

$$\text{Pf}(iX_{\pm}\Gamma) = \text{Pf}\left(\begin{bmatrix} 0 & \pm 1 \\ \mp 1 & 0 \end{bmatrix}\right) = \pm 1.$$

On the other hand

$$\begin{bmatrix} \cos(t) & 0 & 0 & \sin(t) \\ 0 & \cos(t) & -\sin(t) & 0 \\ 0 & -\sin(t) & \cos(t) & 0 \\ \sin(t) & 0 & 0 & \cos(t) \end{bmatrix}$$

is a real, self-dual, Hermitian unitary path from I_4 to $-I_4$.

4.5. **Class CII, 1D.** This is much like the BDI situation. On $\mathbf{M}_{4n}(\mathbb{C})$ the operation corresponding to particle-charge conjugation is

$$\begin{bmatrix} A & B \\ C & D \end{bmatrix}^\kappa = \begin{bmatrix} A^\# & C^\# \\ B^\# & D^\# \end{bmatrix}.$$

The grading operator is

$$\Gamma = \begin{bmatrix} I & 0 \\ 0 & -I \end{bmatrix}.$$

The operations corresponding to time-reversal is

$$\begin{aligned} \begin{bmatrix} A & B \\ C & D \end{bmatrix}^\tau &= \begin{bmatrix} I & 0 \\ 0 & -I \end{bmatrix} \begin{bmatrix} A & B \\ C & D \end{bmatrix}^\kappa \begin{bmatrix} I & 0 \\ 0 & -I \end{bmatrix} \\ &= \begin{bmatrix} I & 0 \\ 0 & -I \end{bmatrix} \begin{bmatrix} A^\# & C^\# \\ B^\# & D^\# \end{bmatrix} \begin{bmatrix} I & 0 \\ 0 & -I \end{bmatrix} \\ &= \begin{bmatrix} A^\# & -C^\# \\ -B^\# & D^\# \end{bmatrix}. \end{aligned}$$

To check these are the correct type, we notice

$$\begin{bmatrix} A & B \\ C & D \end{bmatrix}^\kappa = - \begin{bmatrix} Z & 0 \\ 0 & Z \end{bmatrix} \begin{bmatrix} A & B \\ C & D \end{bmatrix}^T \begin{bmatrix} Z & 0 \\ 0 & Z \end{bmatrix}$$

and

$$\begin{bmatrix} A & B \\ C & D \end{bmatrix}^\tau = - \begin{bmatrix} Z & 0 \\ 0 & -Z \end{bmatrix} \begin{bmatrix} A & B \\ C & D \end{bmatrix}^T \begin{bmatrix} Z & 0 \\ 0 & -Z \end{bmatrix},$$

and since

$$\begin{bmatrix} Z & 0 \\ 0 & Z \end{bmatrix}^2 = \begin{bmatrix} Z & 0 \\ 0 & -Z \end{bmatrix}^2 = - \begin{bmatrix} I & 0 \\ 0 & I \end{bmatrix}$$

we have $\mathcal{C} \circ \mathcal{C} = -I$ and $\mathcal{T} \circ \mathcal{T} = -I$.

Our matrices are Hermitian X and H with X even and $X^\kappa = X$, and with H odd and $H^\kappa = H$. The index we use is

$$\frac{1}{4} \text{Sig}(X\Gamma + H).$$

The reason for the extra factor of one-half will be evident from the symmetries here. We note

$$(X\Gamma + H)^* = \Gamma X + H = X\Gamma + H$$

and

$$(X\Gamma + H)^\tau = \Gamma^\tau X + H = \Gamma X + H = X\Gamma + H$$

so this matrix is “self-dual” and Hermitian, so has Kramer’s doubling.

Arguing as before, we reduce to the case $H = 0$ and X unitary. This means

$$X = \begin{bmatrix} Y & \\ & Z \end{bmatrix}$$

with Y and Z both self-dual, Hermitian and unitary. Since

$$\frac{1}{4}\text{Sig}(X\Gamma) = \frac{1}{4}\text{Sig}\begin{bmatrix} Y & \\ & -Z \end{bmatrix} = \frac{1}{4}\text{Sig}(Y) - \frac{1}{4}\text{Sig}(Z)$$

we initially seem to be short by one invariant. The path

$$U_t = \begin{bmatrix} \cos(t) & & \sin(t) & \\ & \cos(t) & & \sin(t) \\ \sin(t) & & -\cos(t) & \\ & \sin(t) & & -\cos(t) \end{bmatrix}$$

illustrates how to use nonzero H_t to increase one signature by four while decreasing the other by four.

5. DIMENSION TWO, INDEX FORMULAS

What we are after here are invariants that, for two dimensional finite systems on a square, can be quickly computed and that can explain the robustness of gapless edge modes in the face of disorder. We only consider disorder that respects the symmetry class. However, the simplicity of these invariants should mean they function well for disorder that is only approximately invariant under the needed symmetries.

5.1. Class A in 2D. We have no reality condition and use the index from Section 1, at the origin, so

$$\frac{1}{2}\text{Sig}(X \otimes \sigma_x + Y \otimes \sigma_y + H \otimes \sigma_z).$$

Notice that if consider

$$H' = X \otimes \sigma_x + Y \otimes \sigma_y + H \otimes \sigma_z$$

as a derived Hamiltonian, it constitutes a class A system in 0D.

5.2. Class D in 2D. We can assume, after perhaps a unitary change of basis, that H is imaginary while X and Y are real, all being Hermitian. We select our Γ_j so that H is tensored with σ_y , which is imaginary. Therefore

$$H' = X \otimes \sigma_z + Y \otimes \sigma_x + H \otimes \sigma_y = \begin{bmatrix} X & Y - iH \\ Y + iH & X \end{bmatrix}$$

defines a 0D system in class AI. That is, it is real symmetric and, by the local gap assumption, invertible. In terms of Table 2 this moves us two steps up and two to the left. This is similar to the scattering matrix approach of Fulga et al. [14] which, in slightly different geometry, moves one step up and one step left.

We utilize the invariant from Class AI in 0D and use

$$\frac{1}{2}\text{Sig}(X \otimes \sigma_z + Y \otimes \sigma_x + H \otimes \sigma_y).$$

This is invariant under homotopy, is additive with respect to direct sums, and is trivial on trivial systems. It could be the trivial invariant. Perhaps the best way to

show these invariants nontrivial is to use them in an numerical study. We do that in some cases. Here we derive the existence of a nontrivial example mathematically.

The standard example [5, 17] of three almost commuting Hermitian matrices

$$\frac{1}{2} \text{Sig} \begin{bmatrix} X & Y - iH \\ Y + iH & X \end{bmatrix} = \pm 1$$

has one matrix, say H , imaginary and the others real. All we are missing is having X and Y commute. By the class AI version of Lin's Theorem [30] we can modify these a little to produce X_1 and Y_1 that are commuting real orthogonal matrices. If we use a large enough matrix size, $B(X, Y, H)$ will have a large spectral gap, meaning the index will be unchanged when applied to (X_1, Y_1, H) .

5.3. Class DIII in 2D. We are given symmetries $H^\sharp = H$, $X^\sharp = X$ and $Y^\sharp = Y$ on top of knowing X and Y are real and H is imaginary, as in Section 5.2. As we did there, we set

$$H' = X \otimes \sigma_z + Y \otimes \sigma_x + H \otimes \sigma_y.$$

This is real, so $H'^{\text{T} \otimes \text{T}} = H'$, while $H'^{\sharp \otimes \sharp} = H'$. With these symmetry operations, the grading operator is $Z \otimes Z$. We need to select partial isometries into the 1 and -1 eigenspaces for this grading operator, and choose

$$W_+ = \frac{1}{\sqrt{2}} \begin{bmatrix} I & 0 \\ 0 & I \\ 0 & -I \\ I & 0 \end{bmatrix}, \quad W_- = \frac{1}{\sqrt{2}} \begin{bmatrix} I & 0 \\ 0 & I \\ 0 & I \\ -I & 0 \end{bmatrix}.$$

Now we can use the index from Class BDI in dimension zero and define our index as

$$\text{sign}(\det(W_+^* H' W_-)).$$

We want to see this is not a trivial index.

Suppose (X, Y, H) is any example from class D, which can exist with both odd index and even. Let our class DIII example be the $2n$ -by- $2n$ matrices

$$(5.1) \quad X_1 = \begin{bmatrix} X & \\ & X \end{bmatrix}, \quad Y_1 = \begin{bmatrix} Y & \\ & Y \end{bmatrix}, \quad H_1 = \begin{bmatrix} H & \\ & -H \end{bmatrix}.$$

The index is then the sign of the determinant of

$$\begin{aligned} & \frac{1}{2} \begin{bmatrix} I & 0 & 0 & I \\ 0 & I & -I & 0 \end{bmatrix} \begin{bmatrix} X & 0 & Y - iH & 0 \\ 0 & X & 0 & Y + iH \\ Y + iH & 0 & -X & 0 \\ 0 & Y - iH & 0 & -X \end{bmatrix} \begin{bmatrix} I & 0 \\ 0 & I \\ 0 & I \\ -I & 0 \end{bmatrix} \\ &= \begin{bmatrix} X & Y - iH \\ -Y - iH & X \end{bmatrix} \\ &= \begin{bmatrix} I & 0 \\ 0 & -I \end{bmatrix} \begin{bmatrix} X & Y - iH \\ Y + iH & -X \end{bmatrix} \end{aligned}$$

so the

$$\text{ind}(X_1, Y_1, H_1) = (-1)^{\text{ind}(X, Y, H)}.$$

Remark 5.1. Notice that in this example, the index comes out 1 when we start with X and Y and H all commuting. An easy homotopy argument shows we get trivial index of 1 whenever we start in class DIII with all three matrices commuting. This means we made valid choices for W_{\pm} .

5.4. Class AII in 2D. We have one symmetry $H^{\sharp} = H$, $X^{\sharp} = X$ and $Y^{\sharp} = Y$. We set

$$H' = X \otimes \sigma_x + Y \otimes \sigma_y + H \otimes \sigma_z$$

and find $H'^{\sharp \otimes \sharp} = -H'$. We are in a nonstandard version of class D, dimension zero. The unitary matrix

$$Q = \frac{1}{\sqrt{2}} \begin{bmatrix} I & -iZ \\ iZ & I \end{bmatrix} = \frac{1}{\sqrt{2}} \begin{bmatrix} I & 0 & 0 & -iI \\ 0 & I & iI & 0 \\ 0 & iI & I & 0 \\ -iI & 0 & 0 & I \end{bmatrix}$$

brings us to the standard picture and our invariant is

$$\text{sign}(\text{Pf}(iQ^*H'Q)).$$

We conduct a numerical study that provides ample evidence that this is not a trivial invariant.

Remark 5.2. There are many choices here, including conventions as to the definition of the Pfaffian, so that it is easy to program this wrong. Done correctly, the index is 1 when H and X and Y all commute.

5.5. Class C in 2D. We have one symmetry $H^{\sharp} = -H$, $X^{\sharp} = X$ and $Y^{\sharp} = Y$. We set

$$H' = X \otimes \sigma_z + Y \otimes \sigma_x + H \otimes \sigma_y$$

so that $H'^{\sharp \otimes \text{T}} = H'$. We are in a nonstandard version of class AII, dimension zero. The matrix

$$Q = \begin{bmatrix} I & 0 & 0 & 0 \\ 0 & 0 & I & 0 \\ 0 & I & 0 & 0 \\ 0 & 0 & 0 & I \end{bmatrix}$$

converts is to the standard dual operation. Our invariant is

$$\frac{1}{4} \text{Sig}(QH'Q) = \frac{1}{4} \text{Sig}(H').$$

To show nontrivial values of this index are possible, consider any example from class D. Let our class C example be

$$(5.2) \quad X_1 = \begin{bmatrix} X & \\ & X \end{bmatrix}, \quad Y_1 = \begin{bmatrix} Y & \\ & Y \end{bmatrix}, \quad H_1 = \begin{bmatrix} H & \\ & H \end{bmatrix}.$$

Then

$$\begin{aligned} QH'Q &= Q \begin{bmatrix} X & 0 & Y - iH & 0 \\ 0 & X & 0 & Y - iH \\ Y + iH & 0 & -X & 0 \\ 0 & Y + iH & 0 & -X \end{bmatrix} Q \\ &= \begin{bmatrix} X & Y - iH & & \\ Y + iH & -X & & \\ & & X & Y - iH \\ & & Y + iH & -X \end{bmatrix} \end{aligned}$$

so

$$\text{ind}_{\mathbb{C}}(X_1, Y_1, H_1) = \text{ind}_{\mathbb{D}}(X, Y, H).$$

6. DIMENSION THREE, INDEX FORMULAS

We believe in all five interesting classes in three dimensions we can move up two and left two in Table 1 and arrive at a useful index. For now, we study this just in Class AII. In this class, we have examples from physics research (with Hastings [18]) to show this invariant is interesting, and theorems about the K -theory of real C^* -algebras (with Boersema [4]) that allow us to identify the invariant.

The higher dimensional invariants in classes just one antiunitary symmetry, can be explained using the theory of real (ungraded) C^* -algebras. This will be discussed elsewhere.

6.1. Class AII in 3D. We have one symmetry $H^\sharp = H, X^\sharp = X, Y^\sharp = Y$, and $Z^\sharp = Z$. We set

$$H' = X \otimes \sigma_x + Y \otimes \sigma_y + Z \otimes \sigma_z$$

and

$$X' = H \otimes I$$

and find and find $H'^{\sharp \otimes \sharp} = -H'$ and $X'^{\sharp \otimes \sharp} = X'$ so we have a derived 1D system in class D. The unitary matrix

$$Q = \frac{1}{\sqrt{2}} \begin{bmatrix} I & 0 & 0 & -iI \\ 0 & I & iI & 0 \\ 0 & iI & I & 0 \\ -iI & 0 & 0 & I \end{bmatrix}$$

brings us to the standard picture and our invariant is

$$\text{sign}(\det(Q^*(X' + iH')Q)) = \text{sign}(\det(X' + iH')).$$

Again we offer a numerical study that provides ample evidence that this is not the trivial invariant.

Remark 6.1. The advantage of the left form of the invariant is that an LU factorization will be faster and take less memory.

7. BULK-EDGE CORRESPONDENCE

We now prove a relation between the index values in the pseudoresolvent and the pseudospectrum. Essentially, between two points in energy-position space where the index changes, there must be a point in the pseudospectrum. So at that point there must be a vector approximately localized in position and energy. For weak disorder, this will mean a vector localized at the edge and localized at the Fermi level. For strong disorder, things get messier, with the “edge modes” forming a ring around the sample, sometimes moved in from the edge.

Unlike in [12] and [20], for example, we do not have a separate Hamiltonian for the edge states. Rather we are classifying the approximate zero modes of the Hamiltonian. In a system with weak disorder and nontrivial invariant in the center, these approximate zero modes cannot localize in the bulk, but they can and do localize near the edge. Since the value of the invariant is robust against disorder, at least disorder with the correct symmetry, whatever is happening at the edge is robust.

We are not claiming the converse. Most likely, in higher dimensions there are robust edge effects that can exist without these particular invariants being nonzero. Indeed, see the discussion of stabilization in K -theory in [23].

We will use $\text{ind}(X_1, \dots, X_{D+1})$ generically for any of the indices described on Sections 3-6. We do not assume in this section that the first D matrices commute. Our convention is to call X_{D+1} the Hamiltonian, even if these matrices are not related to quantum systems.

We will assume the needed symmetries on the Γ_j to correspond to the choices made in the definition of a specific index. For example when $D = 3$ and we are in Class AII, the index is

$$(7.1) \quad \text{sign} \left(\det \left(Q^* \begin{bmatrix} 0 & 0 & H+iZ & iX+Y \\ 0 & 0 & iX-Y & H-iZ \\ H-iZ & -iX-Y & 0 & 0 \\ -iX+Y & H+iZ & 0 & 0 \end{bmatrix} Q \right) \right)$$

so our choices for the $\Gamma_1, \Gamma_2, \Gamma_3, \Gamma_4$ are

$$\begin{bmatrix} 0 & 0 & 0 & i \\ 0 & 0 & i & 0 \\ 0 & -i & 0 & 0 \\ -i & 0 & 0 & 0 \end{bmatrix}, \quad \begin{bmatrix} 0 & 0 & 0 & 1 \\ 0 & 0 & -1 & 0 \\ 0 & -1 & 0 & 0 \\ 1 & 0 & 0 & 0 \end{bmatrix}, \quad \begin{bmatrix} 0 & 0 & i & 0 \\ 0 & 0 & 0 & -i \\ -i & 0 & 0 & 0 \\ 0 & i & 0 & 0 \end{bmatrix}, \quad \begin{bmatrix} 0 & 0 & 1 & 0 \\ 0 & 0 & 0 & 1 \\ 1 & 0 & 0 & 0 \\ 0 & 1 & 0 & 0 \end{bmatrix}.$$

What is essential is that the index can be computed continuously from

$$B(X_1, \dots, X_{D+1})$$

whenever this is invertible. This means that given a continuous path

$$(X_{1,t}, \dots, X_{D+1,t})$$

the only way for to change is for it to be undefined at some point because

$$B(X_{1,t}, \dots, X_{D+1,t})$$

is singular.

Definition 7.1. Assume (X_1, \dots, X_{D+1}) are in some symmetry class. If that symmetry class does not have any symmetry that anticommute with the Hamiltonian, then for any $(D + 1)$ -tuple λ not in $\Lambda(X_1, \dots, X_{D+1})$ define

$$\text{ind}_\lambda(X_1, \dots, X_{D+1}) = \text{ind}(X_1 - \lambda_1 I, \dots, X_{D+1} - \lambda_{D+1} I).$$

In the other classes, we do the same except only define this index at a point λ when $\lambda_{D+1} = 0$.

Lemma 7.2. *If (X_1, \dots, X_{D+1}) and (Y_1, \dots, Y_{D+1}) are tuples of Hermitian matrices of the same size then*

$$\left| \|(B(X_1, \dots, X_{D+1}))^{-1}\|^{-1} - \|(B(Y_1, \dots, Y_{D+1}))^{-1}\|^{-1} \right| \leq \sqrt{\sum \|X_j - Y_j\|^2}.$$

If (X_1, \dots, X_{D+1}) and (Y_1, \dots, Y_{D+1}) are in the same symmetry class and

$$\text{ind}(X_1, \dots, X_{D+1}) \neq \text{ind}(Y_1, \dots, Y_{D+1})$$

then

$$\left| \|(B(X_1, \dots, X_{D+1}))^{-1}\|^{-1} + \|(B(Y_1, \dots, Y_{D+1}))^{-1}\|^{-1} \right| \leq \sqrt{\sum \|X_j - Y_j\|^2}$$

and somewhere on the line segment $(X_{1,t}, \dots, X_{D+1,t})$ between these pairs is a point where

$$B(X_{1,t}, \dots, X_{D+1,t})$$

is singular.

Proof. We apply Weyl's estimate on the spectral variation of Hermitian matrices to

$$B(X_{1,t}, \dots, X_{D+1,t})$$

at various places along the line defined by

$$X_{j,t} = (1 - t)X_j + Y_j.$$

Let's let a be the eigenvalue of smallest magnitude for $B(X_1, \dots, X_{D+1})$, so

$$a = \pm \|(B(X_1, \dots, X_{D+1}))^{-1}\|^{-1}$$

and similarly have an eigenvalue b for $B(Y_1, \dots, Y_{D+1})$ with

$$b = \pm \|(B(Y_1, \dots, Y_{D+1}))^{-1}\|^{-1}.$$

Without loss of generality, $|a| < |b|$. The closest eigenvalue to a in the spectrum of $B(Y_1, \dots, Y_{D+1})$ is at least at a distance of $|b| - |a|$ away. This is then a lower bound on the best overall spectral pairing, and that in turn a lower bound on the distance between the matrices.

If the index varies, then at some t the matrix

$$B(X_{1,t}, \dots, X_{D+1,t})$$

is singular, since the index is continuous where defined. We can apply the first statement in the result to $B(X_1, \dots, X_{D+1})$ and $B(X_{1,t}, \dots, X_{D+1,t})$, and then again to $B(Y_1, \dots, Y_{D+1})$ and $B(X_{1,t}, \dots, X_{D+1,t})$. These points are collinear so the estimates add. \square

Lemma 7.3. *For any two $(D+1)$ -tuples $\boldsymbol{\lambda}$ and $\boldsymbol{\mu}$ of scalars,*

$$\|B(\lambda_1 I, \dots, \lambda_{D+1} I) - B(\mu_1 I, \dots, \mu_{D+1} I)\| = d(\boldsymbol{\lambda}, \boldsymbol{\mu})$$

where d denotes Euclidean distance.

Proof. We first notice

$$B(\lambda_1 I, \dots, \lambda_{D+1} I) - B(\mu_1 I, \dots, \mu_{D+1} I) = B((\lambda_1 - \mu_1) I, \dots, (\lambda_{D+1} - \mu_{D+1}) I)$$

so we need only compute

$$\|B(\mu_1 I, \dots, \mu_{D+1} I)\|.$$

By Equation 1.2,

$$B(\gamma_1 I, \dots, \gamma_{D+1} I)^2 = \sum \gamma_j^2 I$$

so, by the spectral mapping theorem,

$$\sigma(B(\gamma_1 I, \dots, \gamma_{D+1} I)) \subseteq \left\{ \pm \sqrt{\sum \gamma_j^2} \right\}.$$

Therefore

$$\|B(\gamma_1 I, \dots, \gamma_{D+1} I)\| = \sqrt{\sum \gamma_j^2}.$$

\square

So now we know that points in the pseudospectrum with different index must be separated by certain distance. We also have a means to estimate how much disorder is needed to change an index. The reason nonzero index is thus important, when it is found, is that trivial index prevails away from the origin.

Lemma 7.4. *If (X_1, \dots, X_{D+1}) is in any symmetry class, and if*

$$|\boldsymbol{\lambda}| > \|B(X_1, \dots, X_{D+1})\|$$

then $\boldsymbol{\lambda}$ is in the pseudoresolvent and

$$\text{ind}_{\boldsymbol{\lambda}}(X_1, \dots, X_{D+1}) = 0.$$

Proof. Notice first that $B(\lambda_1 I, \dots, \lambda_{D+1} I)$ has spectrum $\{\pm |\boldsymbol{\lambda}|\}$ with trivial index, in any symmetry class. We then consider the path $B_{\boldsymbol{\lambda}}(tX_1, \dots, tX_{D+1})$ which has length

$$\|B(X_1, \dots, X_{D+1})\|.$$

For the signature along this path to change, it will need to be at least as long as $|\boldsymbol{\lambda}|$. \square

We now prove bulk-edge correspondence. To accommodate highly disordered systems, we allow for a generous interpretation of edge mode. A nontrivial index in the center will need to be surrounded, but not too closely, by a ring of approximate modes approximately at the Fermi level (assumed here to be zero). We can, for less disordered systems, compute the index well away from the center and see that the edge modes are really near the edge.

Theorem 7.5. *Suppose (X_1, \dots, X_D, H) is in any symmetry class and that*

$$\text{ind}(X_1, \dots, X_D, H)$$

is nontrivial and

$$R = \|(B(X_1, \dots, X_D, H))^{-1}\|^{-1}$$

is positive. Then for every unit D -tuple $(\alpha_1, \dots, \alpha_D)$, at some point along the ray

$$t \mapsto \boldsymbol{\lambda}_t = (t\alpha_1, \dots, t\alpha_D, 0)$$

there is a $\boldsymbol{\lambda}_s$ which is in the pseudospectrum. If $\boldsymbol{\lambda}_t$ is in the pseudospectrum then

$$R \leq |\boldsymbol{\lambda}_t| \leq \sqrt{\|H\|^2 + \sum_j \|X_j\|^2 + \sum_j \|[X_j, H]\| ..}$$

Proof. Suppose $\boldsymbol{\lambda}_t$ is in the pseudospectrum. The claim $|\boldsymbol{\lambda}_t| \geq R$ follows directly from Lemmas 7.2 and 7.3. We know from Lemma 7.4 that $\boldsymbol{\lambda}_t$ is in the pseudoresolvent whenever

$$|\boldsymbol{\lambda}_t| > \|B(X_1, \dots, X_D, H)\|.$$

We now use Equation 1.2 to get a bound on this norm,

$$\begin{aligned} \|B(X_1, \dots, X_D, H)\|^2 &= \|B(X_1, \dots, X_D, H)^2\| \\ &\leq \left\| H^2 + \sum X_j^2 \right\| + \left\| \sum [X_j, H] \right\| \\ &\leq \|H\|^2 + \sum \|X_j\|^2 + \sum \|[X_j, H]\|. \end{aligned}$$

If $\boldsymbol{\lambda}_t$ is in the pseudospectrum then

$$|\boldsymbol{\lambda}_t|^2 \leq \|H\|^2 + \sum \|X_j\|^2 + \sum \|[X_j, H]\|.$$

Again using Lemma 7.4 we see that somewhere on this ray the index is trivial. At the start of the ray the index was assumed to be nontrivial, so Lemma 7.2 tells us that at least one point on the ray is in the pseudospectrum. \square

Remark 7.6. In the symmetry classes without particle-hole conjugation, we can consider rays that slant up or down in the energy direction. In those classes, the edge modes persist above and below the Fermi level. So when $D = 2$ in a class like AII, the pseudospectrum contains a sphere that surrounds a hole. So starting with lattice geometry of a square, we have produced a modified sphere and nontrivial topology.

8. LOCAL AND GLOBAL INVARIANTS

Suppose we have increasing system sizes, say (X_k, Y_k, H_k) with consistent spacial units, such as nanometers. We then must select rescaling of units $\eta_k > 0$ for all k and so work with the observables $(\eta X_k, \eta Y_k, H_k)$. Another view point is that we will be basing our pseudospectrum and index on

$$B(\eta_k X_k, \eta_k Y, H) - B(\eta_k \lambda_1 I, \eta_k \lambda_2 I, \lambda_3 I).$$

In terms of approximate modes, this means we are producing \mathbf{v} that more or less minimize

$$\max(\eta_k \|X_k \mathbf{v} - \lambda_1 \mathbf{v}\|, \eta_k \|Y_k \mathbf{v} - \lambda_2 \mathbf{v}\|, \|H_k \mathbf{v} - \lambda_3 \mathbf{v}\|)$$

which, for points in the pseudospectrum, will be on the order of

$$\sqrt{\eta_k} \sqrt{\| [H_k, X_k] \|, \| [H_k, Y_k] \|}.$$

I.e.

$$\max \left(\sqrt{\eta_k} \|X_k \mathbf{v} - \lambda_1 \mathbf{v}\|, \sqrt{\eta_k} \|Y_k \mathbf{v} - \lambda_2 \mathbf{v}\|, \frac{1}{\sqrt{\eta_k}} \|H_k \mathbf{v} - \lambda_3 \mathbf{v}\| \right) \approx C$$

If we are trying to model a local probe, we would then want to keep η_k constant. Ideally it would be set to correspond to modes localized in energy so most energy spectrum can fit in the band gap of the clean periodic Hamiltonian and with spread in position of a few nanometers. This will correspond to the expected spacial resolution of a scanning tunneling spectroscopy. If we hold η_k constant we will have a *local index* and local pseudospectrum.

If we instead think bulk-edge correspondence, as in Theorem 7.5, then we want

$$R_k = \frac{1}{\eta_k} \left\| (B(\eta_k X_k, \eta_k Y_k, H_k))^{-1} \right\|^{-1}$$

to grow proportionate to $\|X_k\|$ which, for simplicity, we take equal to $\|Y_k\|$. At the very least, we want this to grow, so we need $\eta_k \searrow 0$. In keeping with how we rescale the periodic observables in the torus geometry, we use $\eta_k = \eta_0 / \|X_k\|$ and call the resulting index a *global index*.

9. DIMENSION TWO, NUMERICS

We present examples in two symmetry classes, AI and AII. We look at examples illustrating the local invariant, and do a study of the disorder-averaged global invariant, looking for the type of phase transition out of topological insulator caused by doping. We use Hamiltonians previously used in such studies so we can test the new algorithms.

We have collected ample evidence that the new indices correspond to old indices, in three combinations of dimension and symmetry classes, in the special case of modest disorder strength and where the Fermi level is in the middle of the gap of the periodic Hamiltonian of clean system. We also get equality for trivial systems, meaning systems in the atomic limit. What can we expect to prove here?

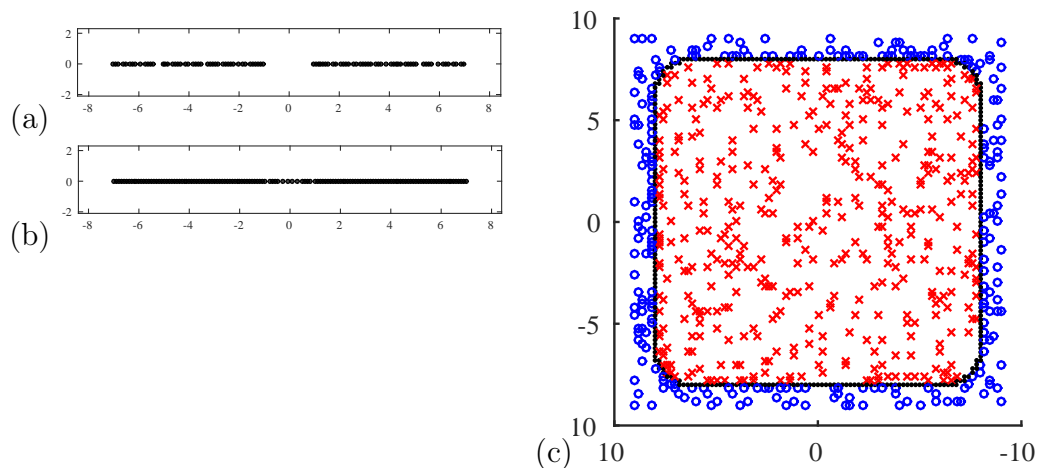


FIGURE 9.1. Chern insulator with zero disorder, looking down at the pseudospectrum and labeled pseudoresolvent at the Fermi level. Panel (a) is the 0.1-pseudospectrum of the Hamiltonian with periodic boundary conditions. Panel (b) is the 0.1-pseudospectrum of the Hamiltonian with zero boundary conditions. Panel (c) is the Clifford pseudospectrum with K -theory labels in the gaps, but only at the Fermi level of zero.

We are discussing invariants that take discrete values on individual finite systems. These are closely related to the K -theory obstructions to fixing approximate matrix representations of C^* -algebra relations to be exact representations [9]. Based on that older research, and the more recent work [28], we expect to soon find a rigorous proof that the new index formulas agree with some established index in the case of weak disorder and with the Fermi level in the middle of a big bulk gap. For the more interesting situation, exploring transitions between topological and ordinary insulating states, we expect at best a probabilistic result. Moreover different indices will mark the transitions differently. We hope to have established a connection with these new indices and edge modes, and the practicality of working with systems of nontrivial size. It will take time to do numerical studies contrasting the phase transitions as found by various index algorithms, including [32, 34] and [14, 15].

9.1. Class AI in 2D. We look again at the model Chern insulator as in Example 1.10. We create the usual Hamiltonian H_{per} with periodic boundary conditions as well as H , the Hamiltonian with zero at the square boundary. We look now at the ϵ -pseudospectrum only at energy zero and compute the local index, using $\eta = 0.02$ and $\epsilon = 0.05$. For comparison we compute the spectrum of both H and H_{per} . In fact we plot the ϵ -pseudospectrum for small ϵ as this is known to close to the actual spectrum and is much faster to compute.

We look at an 18-by-18 lattice with increasing disorder, in Figures 9.1-9.4. At the high value of disorder substantially, as in Figure 9.4, the zero modes have, in places,

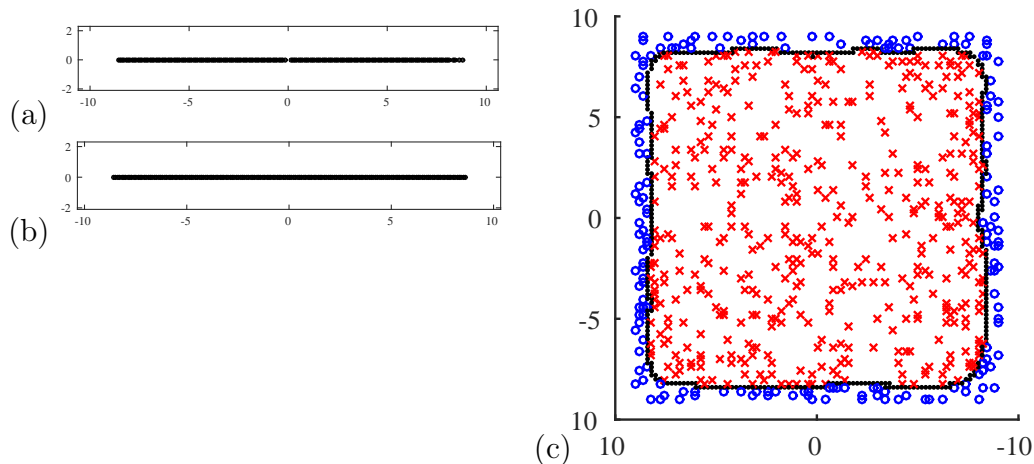


FIGURE 9.2. Chern insulator with disorder set at 7. Panel (a) is the 0.1-pseudospectrum of the Hamiltonian with periodic boundary conditions. Panel (b) is the 0.1-pseudospectrum of the Hamiltonian with zero boundary conditions. Panel (c) is the Clifford pseudospectrum with K -theory labels in the gaps. The bulk gap is just closing at this disorder strength. The small dots (black) are in the pseudospectrum. Some of the grid points in the pseudoresolvent are labeled by their index, with crosses (red) indicating index 1 and with circles (blue) indicating index -1 .

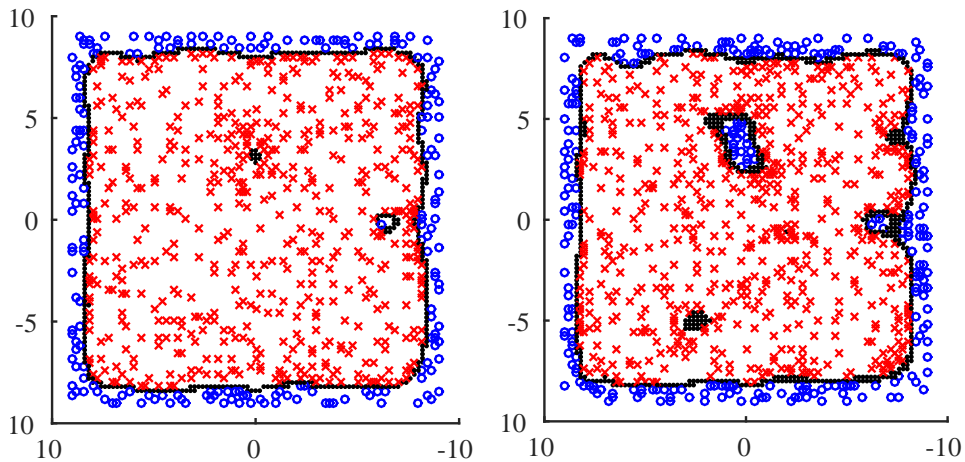


FIGURE 9.3. Chern insulator with disorder set to 8 (left) or 9 (right).

moved in substantially from the edge. On a 50-by-50, in Figure 9.5, we see better how the center of the sample has roughly circular patches of the wrong index, while the corner of the sample still has some semblance of a boundary effect.

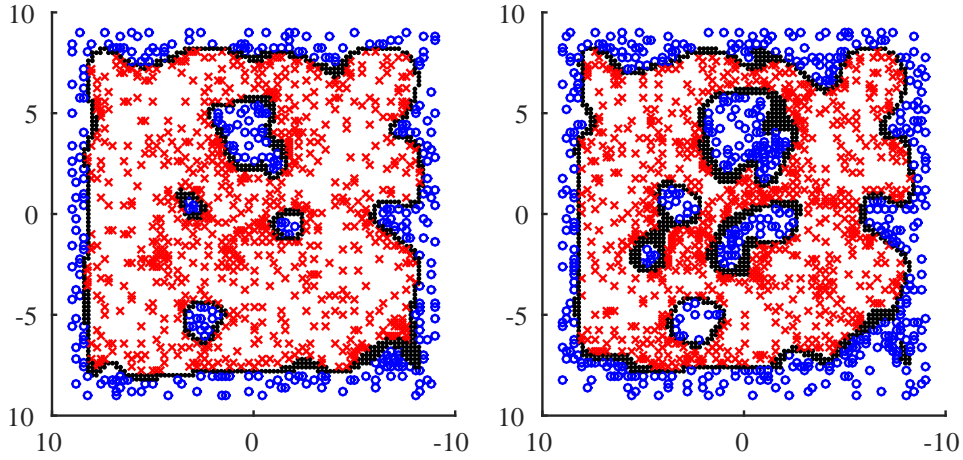


FIGURE 9.4. Chern insulator with disorder set to 10 (left) or 11 (right).

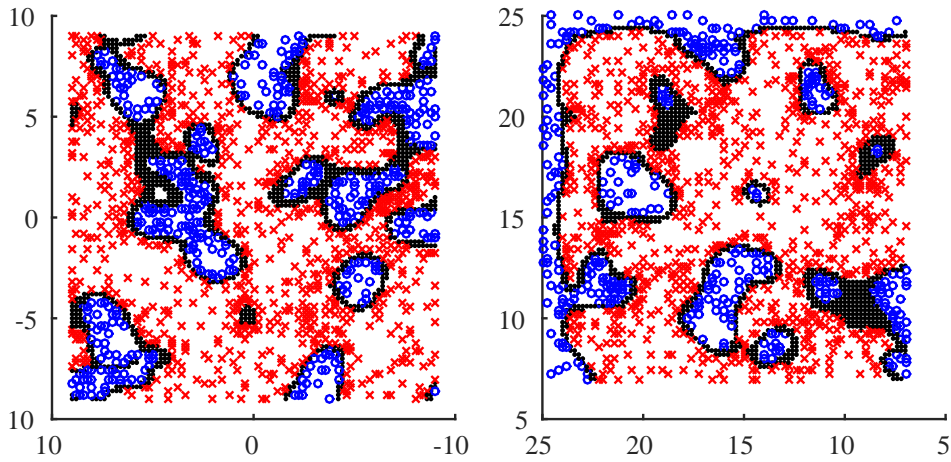


FIGURE 9.5. Chern insulator with disorder set to 11. Now on an 50-by-50 lattice, just in the middle (left) and at the top-right corner (right).

Now we look at the global invariant with $\eta = 4/L$ when the model is on an L -by- L lattice. Holding disorder fixed at 8 we compute the index at the center, but with the energy level moving between -5 and 0 . The results are shown in Figure 9.7

We did this study with dense matrix methods and the formula for the Bott index, in joint work with Hastings [29]. We re-ran this study in order to compute the following proxy for the inverse of spread of the Fermi projector $P = P_{E_F}$,

$$(9.1) \quad \text{concentration}(P_{E_F}) = 1/\sqrt{\|\eta[\hat{U}, P]\|^2 + \|\eta[\hat{V}, P]\|^2}$$

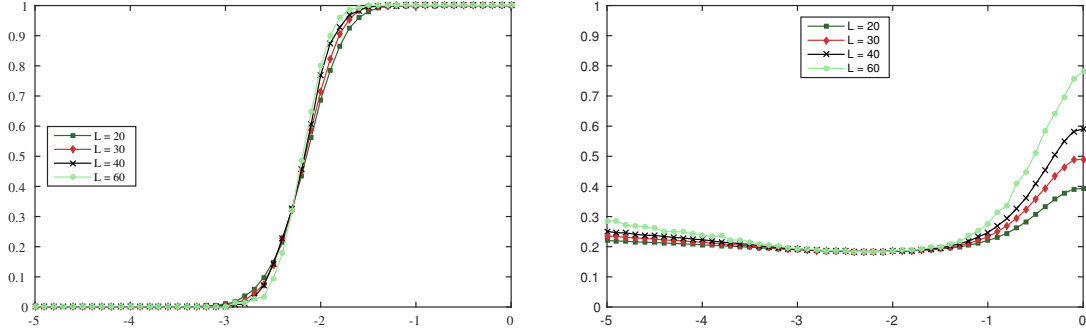


FIGURE 9.6. Chern Insulator by the old Bott index. The number N of samples for an L -by- L lattice used in these averages was: $L = 20$, $N = 10938$; $L = 30$, $N = 2634$; $L = 40$, $N = 1040$; $L = 60$, $N = 150$. The left panel shows the disorder-averaged Bott index with various Fermi levels. The right panel shows the disorder-average of the concentration of the Fermi projector, as defined in Equation 9.1.

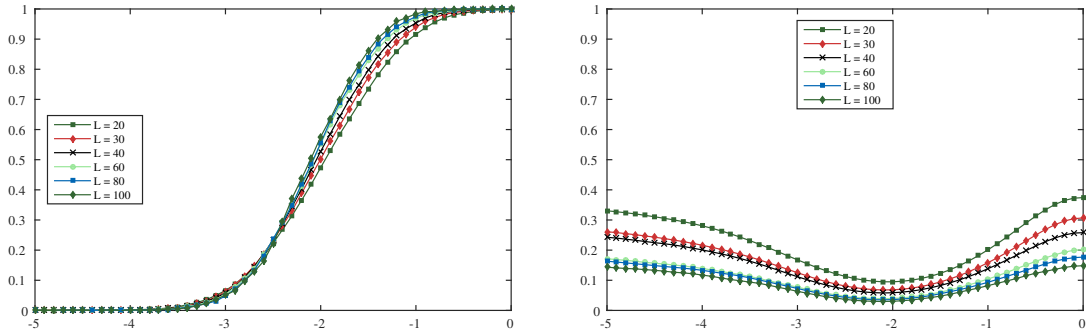


FIGURE 9.7. Chern Insulator by the new index. The number N of samples for an L -by- L lattice used in these averages was: $L = 20$, $N = 15929$; $L = 30$, $N = 21326$; $L = 40$, $N = 16853$; $L = 60$, $N = 10224$; $L = 80$, $N = 8659$; $L = 100$, $N = 2845$. The left panel shows the disorder-averaged new index with various Fermi levels. The right panel shows the disorder-average of gap localized at the origin, as defined in Equation 9.2.

where \hat{U} and \hat{V} are the unitary operators corresponding to "periodic observables" of position on the torus. In terms of the usual position observables X and Y , where we

have

$$\frac{-L+1}{2} \leq X, Y \leq \frac{L-1}{2},$$

we can define these commuting unitary matrices as

$$\hat{U} = e^{\frac{2\pi i}{L}X}, \quad \hat{V} = e^{\frac{2\pi i}{L}Y}.$$

The quantity in Equation 9.1 is expected to be similar to

$$(9.2) \quad \text{localGap}(F) = \left\| (B(\eta X, \eta Y, H - E_F))^{-1} \right\|^{-1}$$

in the new method. It is slow to compute because computing the Fermi projector is slow.

By the Fermi projector we mean the spectral subspace of H_{per} corresponding to $(-\infty, E_F]$. In the event of a large spectral gap we can prove that P will have relatively small commutator with \hat{U} and \hat{V} , as the indicator function can be calculated as $f(H_{\text{per}})$ for f with reasonable Fourier transform. There is also what is called a mobility gap [39], where there is a region of the spectrum around the Fermi level that is filled with eigenvalues that have well localized eigenstates. In that case as well, the commutators $[P, \hat{U}]$ and $[P, \hat{V}]$ tend to be small.

There is an integer we can calculate here, the Bott index. Let $U = P\hat{U}P + (I - P)$ and $V = P\hat{V}P + (I - P)$ and define the index

$$\Re \left(\text{Trace} \left(\frac{1}{2\pi i} \log (VUV^*U^*) \right) \right)$$

which can be proven to be an integer. This integer will be zero when U , V and P are close to a commuting triple of matrices and when it is nonzero such as approximation is precluded. Given a full eigensolve of H_{per} , if assemble all the low-energy eigenstates to form a non-square matrix W with $WW^* = P$, then a reformulation of this formula is

$$\Re \left(\text{Trace} \left(\frac{1}{2\pi i} \log \left(W^* \hat{V} P \hat{U} P \hat{V}^* P \hat{U}^* W \right) \right) \right).$$

We can compute this from just the eigenvalues of $W^* \hat{V} P \hat{U} P \hat{V}^* P \hat{U}^* W$. We do need up to half of the eigenvectors of H_{per} , so an algorithm for the Bott index is easy to implement in $O(n^3)$ time, but no better.

The results using the old method are shown in Figure 9.6. Both methods show a sharpening transition, with the new algorithm able to work with large lattices.

9.2. Class AII in 2D. Now we look at the model used in the the numerical study done with Hastings [29], which was the model for an HgTe quantum well given in [25]. We keep the same disorder and the same strength of the H_{BIA} term that breaks in version symmetry as in the old study [29].

We are just claiming proof of concept, the our formula in a possible replacement for the Pfaffian-Bott index. We can't get to much larger matrices than before because our algorithm to compute the sign of the Pfaffian uses dense matrices. We hope

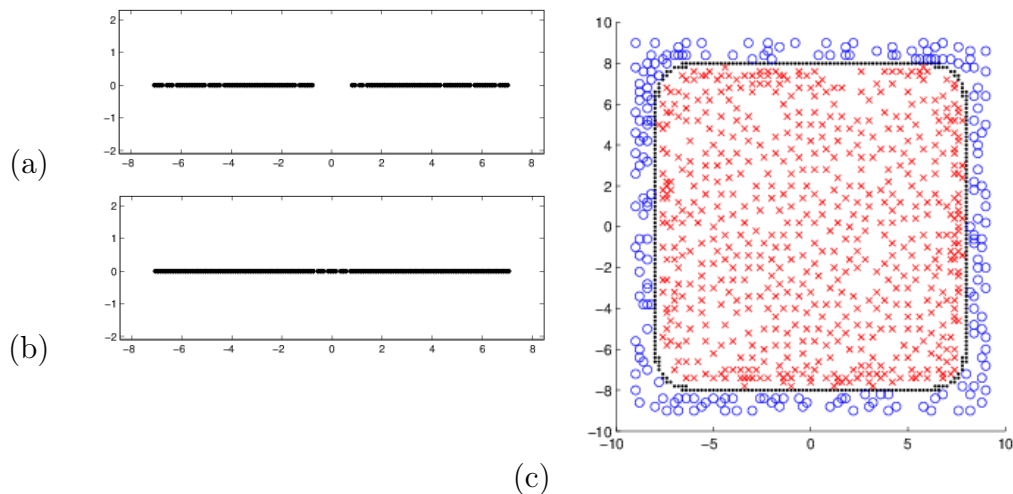


FIGURE 9.8. Class AII insulator with disorder at 0. Panel (a) is the 0.1-pseudospectrum of the Hamiltonian with periodic boundary conditions. Panel (b) is the 0.1-pseudo-spectrum of the Hamiltonian with zero boundary conditions. Panel (c) is the Clifford pseudospectrum with K -theory labels in the gaps.

this data will inspire the production new software implementing the sparse matrix factorization in [8].

We look again at the local index and pseudospectrum, with $\eta = 0.5$. Figures 9.8-9.11 show this with increasing disorder. The red \times indicate index -1 while the blue \circ indicate index 1.

Now the global index. Here we set $\eta = 4/L$ for an L -by- L lattice. Figure 9.12 is reproduced from [29]. We cannot work with larger matrices in this symmetry class because we do not have software to compute the needed factorization of sparse antisymmetric matrices. The results of the new formulas are shown in Figure 9.13. We see that the transition is probably not sharpening as system size increases, but it is hard to tell without the larger system sizes. Notice that 40 lattice units is roughly two nanometers. If we are modeling films of roughly one nanometer thickness, we ought to be looking at $L \approx 200$. Such a size may be in reach of the sparse algorithm as soon as that is available.

10. DIMENSION THREE, NUMERICS

We present examples in one symmetry class, AII.

10.1. Class AII in 3D. The first numerical study [18] in 3D of the effect of doping a topological insulator used an index that worked for periodic boundary conditions. It also involved calculating the sign of a determinant, but involving polynomials in three variables that approximate a degree-one mapping of a three-torus to a three-sphere. The geometry here forces these polynomials to have degree eleven, and the resulting

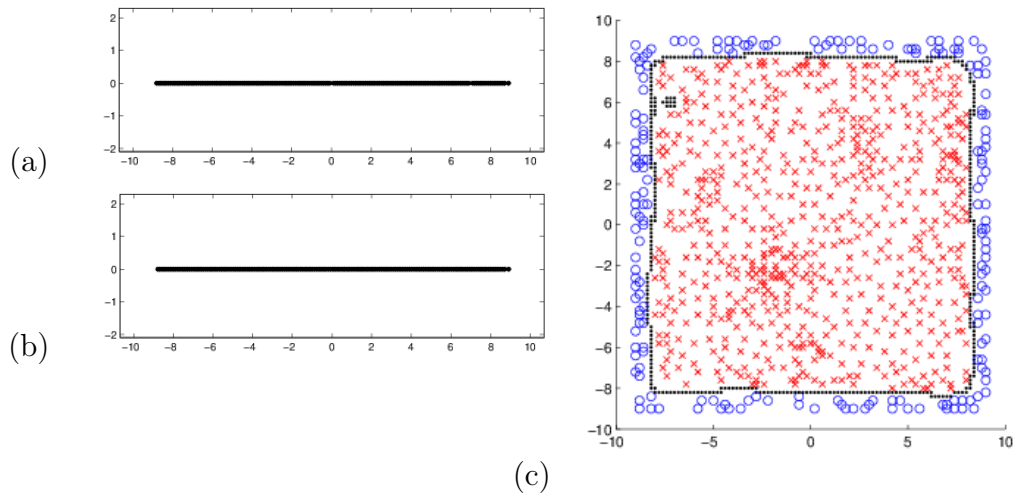


FIGURE 9.9. Class AII insulator with disorder set to 7. Panel (a) is the 0.1-pseudospectrum of the Hamiltonian with periodic boundary conditions. Panel (b) is the 0.1-pseudo-spectrum of the Hamiltonian with zero boundary conditions. Panel (c) is the Clifford pseudospectrum. At this strength of disorder, the bulk gap is just closing.

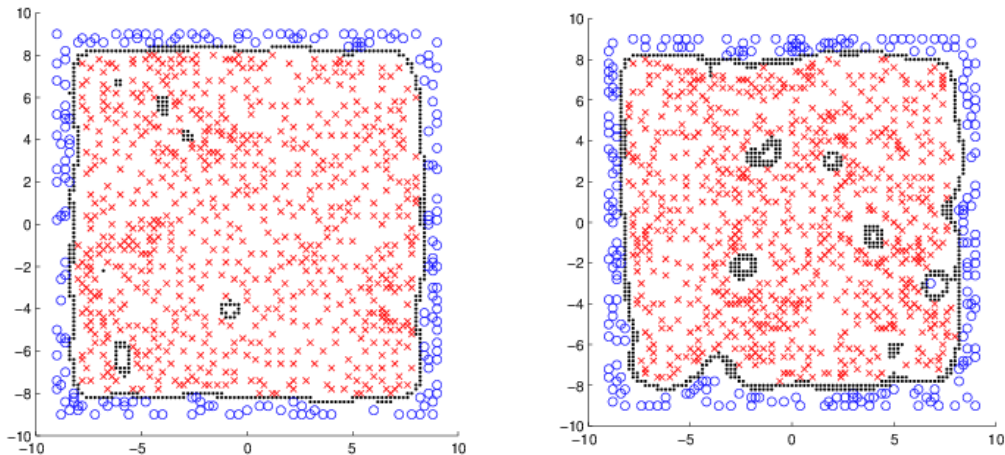


FIGURE 9.10. Class AII insulator with disorder at 8 (left) and 9 (right).

algorithm was slow. In contrast, as we are working with a cube not a three-torus, we have a substantially faster algorithm.

The local index was defined using $\eta = 0.25$. The results are shown in Figures 10.1-10.4. The red \times indicate index -1 while the blue \circ indicate index 1 .

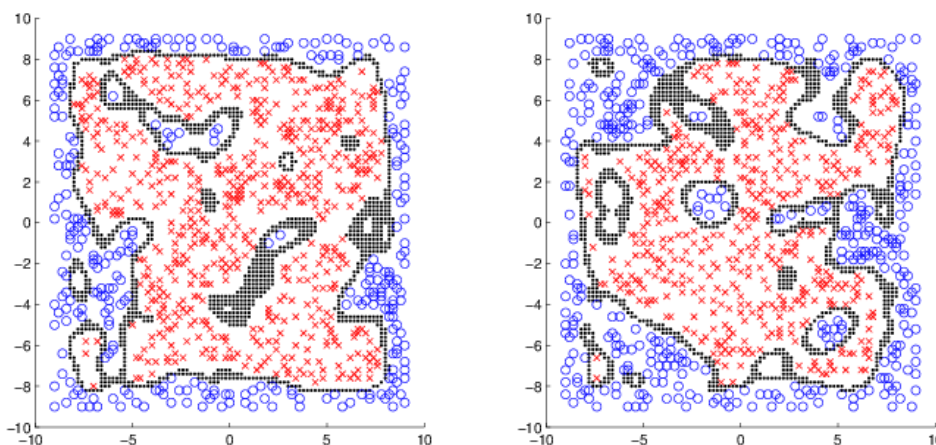


FIGURE 9.11. Class AII insulator with disorder at 10 (left) and 11 (right).

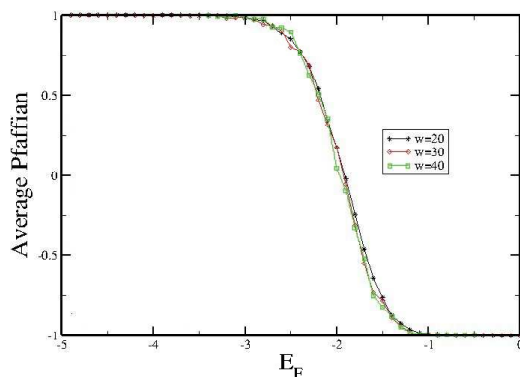


FIGURE 9.12. Phase transition in 2D. The larger plot shows the disorder averaged Pfaffian-Bott index. Reproduced from [29].

The global index was defined using $\eta = 4/L$ for an L -by- L -by- L lattice. Figure 7.2 of [18] is replicated here as Figure 10.5. This data was sufficiently noisy that no real conclusions about scaling could be made. The left panel in Figure 10.6 shows how we can generate much cleaner data with the new algorithm by using more samples and larger systems. It appears now the transition from this 3D topological insulator to an ordinary insulator is not sharp, but larger system sizes are needed to clarify this. These can be studied on existing machines, but the processing time needed will be significant.

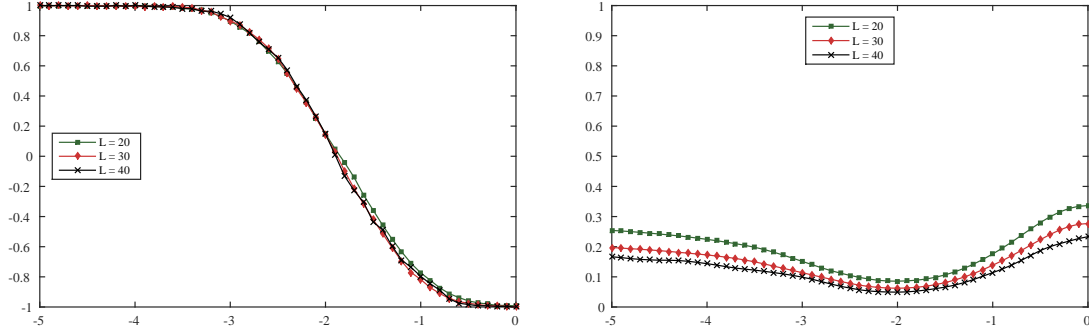


FIGURE 9.13. Phase transition in 2D. The left panel shows the disorder averaged new class AII index. The right panel shows the disorder-average of gap localized at the origin. The number N of samples for an L -by- L lattice used in these averages was: $L = 20$, $N = 3544$; $L = 30$, $N = 2651$; $L = 40$, $N = 481$.

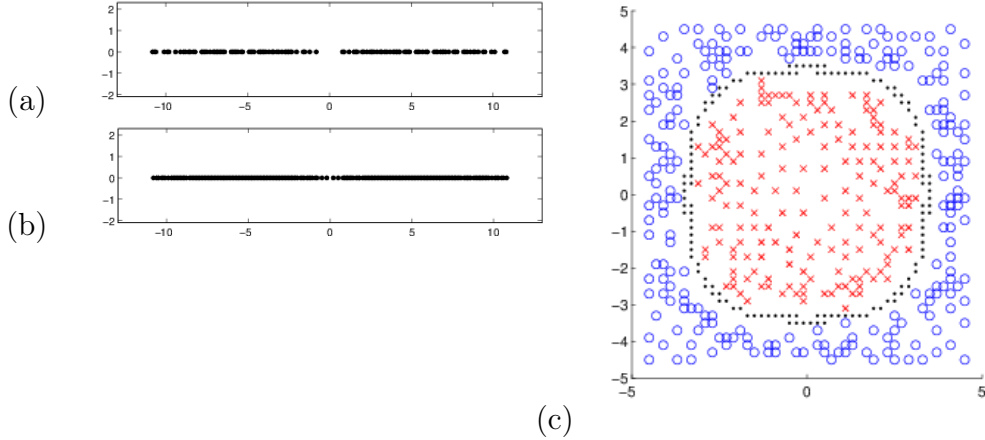


FIGURE 10.1. Class AII insulator in 3D with no disorder. Showing a slice at $z = 0$ and at the Fermi level. Using a 9-by-9-by-9 lattice.

11. THE ALGORITHMS

Matlab code, with instructions on how to produce many of the figures in this paper, will be made available at a data repository¹. For the larger system sizes, the study of the global index was done on multiple computing nodes, each with 32 cores and 64GB of random access memory. However the local index, at the system sizes illustrated in the figures, can be explored using less than a day on a desktop with 4 cores and only 8GB of random access memory.

¹ <https://repository.unm.edu/handle/1928/23449>

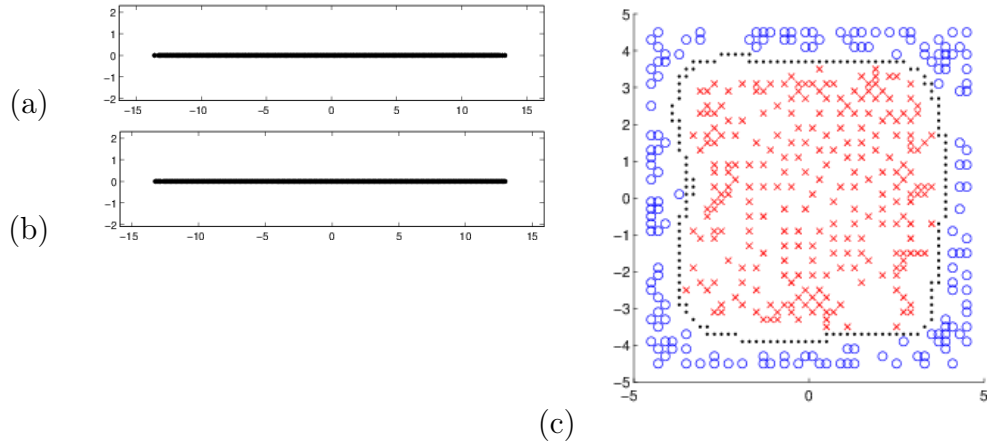


FIGURE 10.2. Class AII insulator in 3D with disorder at 11. Showing a slice at $z = 0$ and at the Fermi level. Using a 9-by-9-by-9 lattice. The bulk gap is just closing at this disorder level.

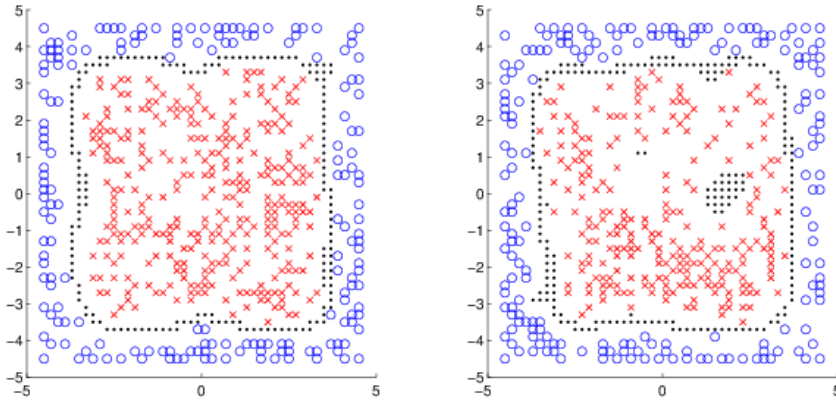


FIGURE 10.3. Class AII insulator in 3D with disorder at 12 (left) and 13 (right).

A good example here is the algorithm for the global class AII invariant in 3D. The formula in equation 7.1 tells us we need to first compute a matrix

$$A = Q^* \begin{bmatrix} 0 & 0 & H + iZ & iX + Y \\ 0 & 0 & iX - Y & H - iZ \\ H - iZ & -iX - Y & 0 & 0 \\ -iX + Y & H + iZ & 0 & 0 \end{bmatrix} Q$$

that is real and sparse. We need to compute its spectral gap

$$\|A^{-1}\|^{-1}$$

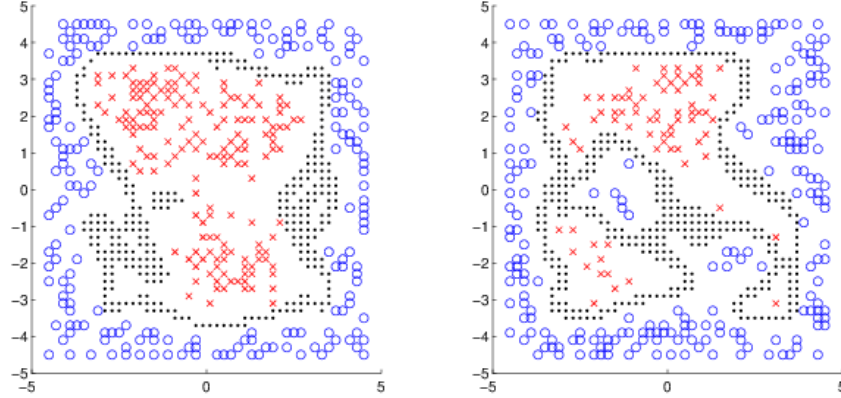


FIGURE 10.4. Class AII insulator in 3D with disorder at 14 (left) and 15 (right).

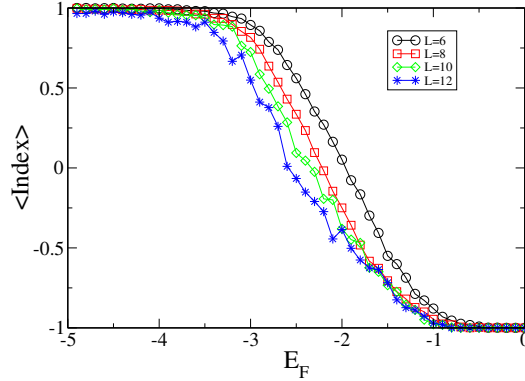


FIGURE 10.5. Phase transition in 3D, as computed via the old method. This figure is replicated from [18]. Shown is a plot of average index for $L = 6, 8, 10, 12$ with $L \times L \times L$ lattices. Each data point is an average of 1700, 1400, 600, 400 samples, respectively.

as well as the sign of its determinant.

We rely on LU algorithm [6], as implemented in Matlab, to factor A as

$$(11.1) \quad A = R^{-1}P^*LUQ^*$$

where R is diagonal, P and Q are permutation matrices, L is lower triangular, sparse with unit diagonal, and U is upper triangular and sparse. The determinant of L is one, and so

$$\text{sign}(\det(A)) = \text{sign}(\det(R))\text{sign}(\det(P))\text{sign}(\det(L))\text{sign}(\det(Q)).$$

These signs of each these determinants is easy to compute. The norm of A^{-1} we compute with the power method. Essentially this method starts with a random unit

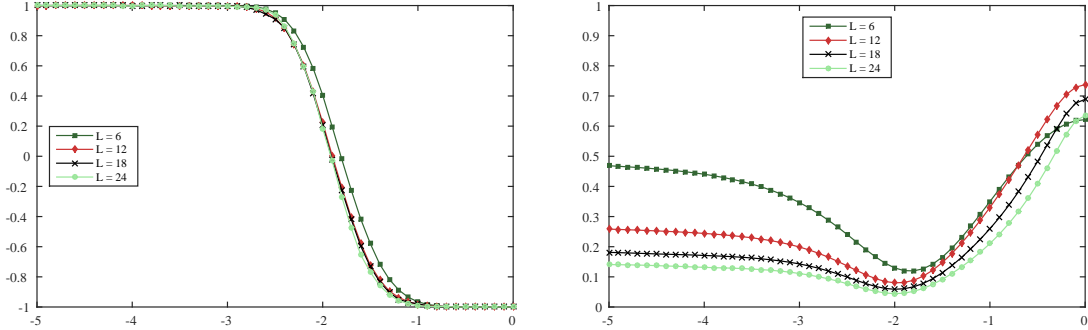


FIGURE 10.6. Phase transition in 3D. The left panel shows the disorder averaged new class AII index. The right panel shows the disorder-average of gap localized at the origin. The number N of samples for an L -by- L -by- L lattice used in these averages was: $L = 6$, $N = 26036$; $L = 12$, $N = 23357$; $L = 18$, $N = 3491$; $L = 24$, $N = 1547$.

vector $\mathbf{v} = \mathbf{v}_0$ and then computes a few dozen iterations of

$$\mathbf{w}_n = (A^*A)^{-1} \mathbf{v}_{n-1}.$$

$$\mathbf{v}_n = \frac{1}{\|\mathbf{w}_n\|} \mathbf{w}_n.$$

We modified this procedure a little. We found starting with \mathbf{v}_0 having all entries equal worked better than a random vector in this setting. Then, following [37], we compute \mathbf{w}_n using equation 11.1 and the Matlab `\` operator that computes $C^{-1}\mathbf{x}$ without inverting the matrix. Since

$$(A^*A)^{-1} = QU^*L^*PR^{-2}P^*LUQ^*,$$

and since $(A^*A)^{-1}$ and $Q^*(A^*A)^{-1}Q$, we can compute \mathbf{w}_n via

$$\mathbf{w}_n = U^* \setminus (L^* \setminus (P \setminus (R^{-2} \setminus (P^* \setminus (L \setminus (U \setminus \mathbf{v}_{n-1})))))).$$

ACKNOWLEDGMENTS

The author wish to thank Deborah Evans, Alexei Kitaev, Matthew Hastings, Joel Moore and Hermann Schulz-Baldes for illuminating discussions, mathematical and physical.

This work was partially supported by a grant from the Simons Foundation (208723 to Loring) and by financial support form the Erwin Schrödinger International Institute for Mathematical Physics. Most of the computing was done on machines at the Center for Advance Research Computing at the University of New Mexico.

REFERENCES

- [1] A. Altland and M.R. Zirnbauer. Nonstandard symmetry classes in mesoscopic normal-superconducting hybrid structures. *Physical Review B*, 55(2):1142, 1997.
- [2] J. Bellissard, A. van Elst, and H. Schulz-Baldes. The noncommutative geometry of the quantum Hall effect. *J. Math. Phys.*, 35(10):5373–5451, 1994.
- [3] David Berenstein and Eric Dzienkowski. Matrix embeddings on flat \mathbb{R}^3 and the geometry of membranes. *Physical Review D*, 86(8):086001, 2012.
- [4] Jeffrey L. Boersema and Terry A. Loring. K -theory for real C^* -algebras via unitary elements with symmetries.
- [5] Man Duen Choi. Almost commuting matrices need not be nearly commuting. *Proc. Amer. Math. Soc.*, 102(3):529–533, 1988.
- [6] Timothy A. Davis and Iain S. Duff. An unsymmetric-pattern multifrontal method for sparse LU factorization. *SIAM J. Matrix Anal. Appl.*, 18(1):140–158, 1997.
- [7] I. S. Duff, N. I. M. Gould, J. K. Reid, J. A. Scott, and K. Turner. The factorization of sparse symmetric indefinite matrices. *IMA J. Numer. Anal.*, 11(2):181–204, 1991.
- [8] Iain S. Duff. The design and use of a sparse direct solver for skew symmetric matrices. *J. Comput. Appl. Math.*, 226(1):50–54, 2009.
- [9] Søren Eilers and Terry A. Loring. Computing contingencies for stable relations. *Internat. J. Math.*, 10(3):301–326, 1999.
- [10] Jean Bellissard Emil Prodan, Bryan Leung. The non-commutative n -th Chern number. arxiv:1305.2425.
- [11] A.M. Essin and JE Moore. Topological insulators beyond the Brillouin zone via Chern parity. *Physical Review B*, 76(16):165307, 2007.
- [12] Andrew M. Essin and Victor Gurarie. Bulk-boundary correspondence of topological insulators from their respective green’s functions. *Phys. Rev. B*, 84:125132, Sep 2011.
- [13] P. Friis and M. Rordam. Almost commuting self-adjoint matrices—a short proof of Huaxin Lin’s theorem. *Journal für die reine und angewandte Mathematik (Crelles Journal)*, 1996(479):121–132, 1996.
- [14] I.C. Fulga, F. Hassler, and A.R. Akhmerov. Scattering theory of topological insulators and superconductors. *Physical Review B*, 85:165409, 2012.
- [15] I.C. Fulga, F. Hassler, A.R. Akhmerov, and C.W.J. Beenakker. Scattering formula for the topological quantum number of a disordered multimode wire. *Physical Review B*, 83(15):155429, 2011.
- [16] M. B. Hastings. Making almost commuting matrices commute. *Communications in Mathematical Physics*, 291(2):321–345, 2009.
- [17] Matthew B. Hastings and Terry A. Loring. Almost commuting matrices, localized Wannier functions, and the quantum Hall effect. *J. Math. Phys.*, 51(1):015214, 2010.
- [18] Matthew B. Hastings and Terry A. Loring. Topological insulators and C^* -algebras: Theory and numerical practice. *Ann. Physics*, 326(7):1699–1759, 2011.
- [19] Ilya Kachkovskiy and Yuri Safarov. On the distance to normal elements in C^* -algebras of real rank zero. *arXiv preprint arXiv:1403.2021*, 2014.
- [20] CL Kane and EJ Mele. \mathbb{Z}_2 topological order and the quantum spin hall effect. *Physical review letters*, 95(14):146802, 2005.
- [21] Vladimir V. Kisil. Möbius transformations and monogenic functional calculus. *Electron. Res. Announc. Amer. Math. Soc.*, 2(1):26–33 (electronic), 1996.
- [22] Alexei Kitaev. Classification of topological insulators and superconductors. Lecture given at the IPMU Focus Week Condensed Matter Physics Meets High Energy Physics, University of Tokyo, 8-12 February 2010.

- [23] Alexei Kitaev. Periodic table for topological insulators and superconductors. In *AIP Conference Proceedings*, volume 1134, page 22, 2009.
- [24] M. König, S. Wiedmann, C. Brune, A. Roth, H. Buhmann, L.W. Molenkamp, X.L. Qi, and S.C. Zhang. Quantum spin Hall insulator state in HgTe quantum wells. *Science*, 318(5851):766, 2007.
- [25] Markus König, Hartmut Buhmann, Laurens W. Molenkamp, Taylor Hughes, Chao-Xing Liu, Xiao-Liang Qi, and Shou-Cheng Zhang. The quantum spin hall effect: theory and experiment. *Journal of the Physical Society of Japan*, 77(3), 2008.
- [26] Huaxin Lin. Almost commuting selfadjoint matrices and applications. In *Operator algebras and their applications (Waterloo, ON, 1994/1995)*, volume 13 of *Fields Inst. Commun.*, pages 193–233. Amer. Math. Soc., Providence, RI, 1997.
- [27] Terry A. Loring. Factorization of matrices of quaternions. *Exposition. Math.*, 30(3):250–267, 2012.
- [28] Terry A. Loring. Quantitative K -theory related to spin Chern numbers. *SIGMA Symmetry Integrability Geom. Methods Appl.*, 10:Paper 077, 25, 2014.
- [29] Terry A. Loring and Matthew B. Hastings. Disordered topological insulators via C^* -algebras. *Europhys. Lett. EPL*, 92:67004, 2010.
- [30] Terry A. Loring and Adam P. W. Sørensen. Almost commuting self-adjoint matrices — the real and self-dual cases. arxiv:1012.3494.
- [31] Terry A. Loring and Adam P. W. Sørensen. Almost commuting orthogonal matrices. *J. Math. Anal. Appl.*, 420(2):1051–1068, 2014.
- [32] Ian Mondragon-Shem, Taylor L. Hughes, Juntao Song, and Emil Prodan. Topological criticality in the chiral-symmetric aiii class at strong disorder. *Phys. Rev. Lett.*, 113:046802, Jul 2014.
- [33] Yoshiko Ogata. Approximating macroscopic observables in quantum spin systems with commuting matrices. *Journal of Functional Analysis*, 2013.
- [34] E. Prodan. Disordered topological insulators: a non-commutative geometry perspective. *Journal of Physics A: Mathematical and Theoretical*, 44:113001, 2011.
- [35] S. Ryu, A.P. Schnyder, A. Furusaki, and A.W.W. Ludwig. Topological insulators and superconductors: tenfold way and dimensional hierarchy. *New Journal of Physics*, 12:065010, 2010.
- [36] Björn Sbierski and Piet W Brouwer. \mathbb{Z}_2 phase diagram of three-dimensional disordered topological insulators via a scattering matrix approach. *Physical Review B*, 89(15):155311, 2014.
- [37] Lloyd N. Trefethen and Mark Embree. *Spectra and pseudospectra*. Princeton University Press, Princeton, NJ, 2005. The behavior of nonnormal matrices and operators.
- [38] M. Wimmer. Efficient numerical computation of the pfaffian for dense and banded skew-symmetric matrices. *ACM Trans. Math. Software*, 38(4), 2012.
- [39] Yan-Yang Zhang, Rui-Lin Chu, Fu-Chun Zhang, and Shun-Qing Shen. Localization and mobility gap in the topological anderson insulator. *Phys. Rev. B*, 85:035107, Jan 2012.

DEPARTMENT OF MATHEMATICS AND STATISTICS, UNIVERSITY OF NEW MEXICO, ALBUQUERQUE, NM 87131, USA.